Article Title

Seismic Loss and Downtime Assessment of Existing Tall Steel-Framed Buildings and Strategies for Increased Resilience

Authors

Carlos Molina Hutt, PE[1], M.ASCE
Ibrahim Almufti, SE[2], M.ASCE
Michael Willford[3]
Gregory Deierlein, PE[4], F.ASCE

Abstract

In areas of high seismicity in the United States, the design of many existing tall buildings followed guidelines that do not provide an explicit understanding of performance during major earthquakes. This paper presents an assessment of the seismic performance of existing tall buildings and strategies for increased resilience for a case study city, San Francisco, where an archetype tall building is designed based on an inventory of the existing tall building stock. A 40-story Moment Resisting Frame (MRF) system is selected as a representative tall building. The archetype building is regular in plan and represents the state of design and construction practice from the mid-1970s to the mid-1980s. Non-Linear Response History Analysis (NLRHA) are conducted with ground motions representative of the design earthquake hazard level defined in current building codes, with explicit consideration of near-fault directivity effects. Mean transient interstory drifts and story accelerations under the 10% in 50 year ground motion hazard range from 0.19% to 1.14% and 0.15g to 0.81g respectively. In order to influence decision making, performance is reported as the expected consequences in terms of direct economic losses and downtime. Furthermore, to achieve increased levels of resilience, a number of strategies are proposed

[1] Teaching Fellow; University College London, Civil, Env. and Geomatic Engineering Dept., Chadwick Building, Gower Street, London, UK, WC1E6BT. Email: carlos.molinahutt@ucl.ac.uk
[2] Associate; Arup, Suite 700, San Francisco, CA, USA, 94105.
[3] Principal, Arup Fellow; Arup, Suite 700, San Francisco, CA, USA, 94105.
[4] Professor; Stanford University, Dept. of Civil and Env. Engineering, Blume Center, Building 540, Stanford, CA, USA, 94305.

including seismic improvements to structural and non-structural systems as well as mitigation measures to minimize impeding factors. Expected direct economic losses for the archetype building are in the order of 34% of building cost and downtime estimates for functional recovery are 87 weeks. The strategies presented in this paper enable up to a 92% reduction in losses and minimize downtime for functional recovery to one day or less.

Subject Headings

Structural Analysis, Seismic Analysis, Non-linear Analysis, Steel Structures, Earthquake Resistant Structures, Resilience, Losses, Downtime

Text

Introduction

Until the introduction of Performance Based Seismic Design (PBSD) in the 1990s, buildings were designed using conventional building codes, which follow a prescriptive force-based approach based on the first mode translational response of the structure (FEMA 2006). Researchers and engineers have raised concerns that the prescriptive approach of building codes is not suitable for tall building design due to the significant contribution of higher mode effects (PEER 2010a). As a result of these shortcomings, several jurisdictions in areas of high seismicity throughout the Unites States (e.g. Los Angeles and San Francisco) have adopted a PBSD approach for the design of new tall buildings. While new designs follow a more adequate approach, little is known about the seismic performance of older existing tall buildings that were designed prior to the adoption of PBSD.

Tall buildings play a key role in the socio-economic activity of major metropolitan areas in the United States. The resilience of these structures is vital in ensuring an effective recovery after major disasters. Events such as the Canterbury earthquake in 2011 have highlighted the impact of poor performing buildings on the business continuity of downtown districts, where tall buildings are typically clustered together. Following the 2011 earthquake, Christchurch's

Central Business District (CBD) red zone covered a significant area of the city and more than 60% of the businesses were displaced (CERC 2012).

This paper presents an assessment of the seismic performance of existing tall buildings in a case study city, San Francisco, where an archetype tall building is designed based on an inventory of the existing tall building stock. The archetype tall building is representative of the state of design and construction practice from the mid-1970s to the mid-1980s. A performance assessment of the archetype building is conducted via NLRHA with ground motions representative of the design earthquake hazard level defined in current building codes and the associated direct economic losses and downtime are estimated from the NLRHA results. Once the performance of the archetype building is assessed, a range of structural and non-structural enhancements are explored for improved performance as well as mitigation measures to minimize downtime.

They key differentiator of the work here presented is that it explicitly considers downtime and recovery in the assessment methodology. This work goes beyond damage and direct losses to consider repair and recovery times. Overall, the main contribution of this paper is that it benchmarks the performance of an archetype tall building considering damage, direct losses (due to repair or replacement), impact on building function and recovery of building function. Furthermore, it evaluates ways of improving resilience by reducing damage and taking other measures to improve recovery. Previous studies have assessed the performance of existing steel moment frame buildings (Muto and Krishnan 2011, Gupta and Krawinkler 1999), but these studies were limited to 20 stories in height and focused on structural performance assessment alone. Other studies have assessed the performance of new tall steel moment frame buildings up to 40 stories (Jayaram and Shome 2012) and estimated economic losses associated with building performance (Shome et al. 2013), but employed simplified single bay two-dimensional structural models that neglect torsional and biaxial effects and do not enable the study of detailed retrofit schemes for enhanced performance. This work draws a comparison of the direct economic loss estimate results for the archetype building and those presented in Shome et al. (2013) for a similar building typology designed to current standards.

Methodology

The Structural Engineers Association of Northern California (SEAONC) Committee on PBSD of Tall Buildings developed an inventory of the existing tall building stock in San Francisco. This committee identified more than 90 buildings of 20 stories or greater, most of which employed a steel moment frame lateral system. In order to assess the seismic performance of existing tall buildings in San Francisco, NLRHA of a representative 40-story building are carried out using the software package LS-DYNA (2013), which accounts for both non-linear material and geometric effects. The three-dimensional analysis employs robust non-linear component models to represent fracture of the welds, flexibility of the panel zones, degradation of the plastic hinges, tensile and flexural capacity of the column splices and buckling of the columns.

Near-fault directivity effects are explicitly considered in the Probabilistic Seismic Hazard Analysis (PSHA) due to the close proximity of active faults to San Francisco's downtown district, where most of these tall buildings are located. Twenty-two ground motion pairs are selected and scaled following a methodology recently implemented for the design of a peer reviewed high rise building in downtown San Francisco (Almufti et al. 2013). Such motions are representative of the design earthquake hazard level defined in current building codes (ASCE 2010) or if expressed in probabilistic terms have 10% chance of occurring over a 50 year period. The selected intensity level is also representative of the "expected earthquake" defined by the San Francisco Planning and Urban Research Association (SPUR) for the purpose of defining resilience. This "expected earthquake" corresponds to a 7.2 earthquake scenario, which is an event that can be expected conservatively, but reasonably within the lifetime of a structure (SPUR 2012).

The United States Federal Emergency Management Agency (FEMA) P-58 Performance Assessment Calculation Tool (PACT) is used in order to assess the probable seismic performance in terms of direct economic losses based on its site, structural, non-structural and occupancy characteristics (FEMA 2012). Conceptual retrofit schemes include structural, non-structural or a combination of these enhancements in order to provide enhanced performance. Structural enhancements schemes include the introduction of an elastic spine throughout the building core with steel bracing and the introduction of base isolation at ground level. Non-structural enhancements introduce building components that are more resilient to earthquake damage. All structural schemes (archetype or baseline, elastic spine and base isolation) are assessed with standard and enhanced non-structural components. Additionally, in order to provide a quantitative measure of resilience, downtime estimates for re-occupancy and functional recovery are reported for all schemes based on the Resilience-based Earthquake Design Initiative (REDi) guidelines (Almufti and Willford 2013).

Since the impact of the schemes considered on the overall resilience of the archetype building is measured in terms of losses and downtime, a brief literature review on loss and downtime assessment as well as resilience quantification is presented. The works referenced are not exhaustive, but are presented to set the context of this work and how it draws and builds on current best practice.

Loss Assessment

In the late 1980s, well founded loss estimation methods began to be employed in the insurance industry and in the 1990s, these were supported by FEMA through the development of the HAZUS earthquake loss estimation software. These developments were primarily directed to the insurance and re-insurance industry (Khater et al. 2002) as HAZUS attempts to address regional impacts of earthquakes. Numerous researchers have since developed approaches to improve loss-estimating methods for individual buildings (Comerio 2006). For instance, Porter and Kiremidjian (2011) proposed a methodology to evaluate the seismic vulnerability of buildings on a building specific basis, which estimates repair cost and repair duration by treating the building as a collection of standard assemblies with probabilistic fragility. Miranda and Aslani (2003) proposed including a probabilistic seismic structural response analysis as a main step in the loss evaluation, enabling the assessment of building specific loss estimation to be expressed probabilistically. These methodologies have been integrated into PBSD of buildings through the FEMA P-58 (2012) project, which enables estimates of direct losses attributable to earthquake damage to an individual building and its contents, as well as the repair or reconstruction time. Unlike previous versions of PBSD, the FEMA P-58 method enables measuring seismic performance through economic losses, which can be understood by decision makers, rather than over methods that report discrete performance levels (Krawinkler and Miranda 2004). Performance is directly related to the damage a building may experience and the consequences of such damage such as loss of use, repair and reconstruction costs (FEMA 2012). The methodology divides the performance assessment into a number of elements that can be resolved rigorously and consistently: earthquake intensity measures, engineering demand parameters, damage measures and decision variables (Moehle and Deierlein 2004).

Downtime Assessment

The main challenge in quantifying downtime are the uncertainties associated with availability of labor, materials, capital and relating damage and repair needs in building components with lack of functionality (Krawinkler and Miranda 2004). The HAZUS method earlier discussed includes a subroutine for calculating downtime. However, this downtime estimate is derived from the direct economic loss estimate. Recognizing this essential component of loss modeling, Comerio (2006) identifies various factors that affect building downtime and divides components contributing to downtime into so-called “rational” and “irrational” components. Rational components are those related to repair work whereas irrational components are those related to resource mobilization. PACT provides an estimate of repair time by combining damage states with probability distributions to represent repair duration. These attempts are aimed at estimating repair time, which is only a small component of overall downtime. More recently, the REDi guidelines propose a detailed downtime assessment methodology by accounting for both direct repairs and impeding factors (analogous to Comerio’s rational and irrational components), where estimates of the different components that contribute to downtime are expressed probabilistically. The REDi guidelines also account for utility disruption in the downtime assessment methodology. Even though utility disruption is an important contributor to downtime, in the present study it does not control over other impeding factors in the overall downtime assessment.

Resilience Quantification

Seismic resilience describes the loss and loss recovery required to maintain the function of a system with minimal disruption (Cimellaro et al. 2006). A resilient system is one that illustrates reduced failure probabilities, reduced consequence from failures (loss of life, damage, etc.) and reduced recovery time (restored functionality) (Bruneau and Reinhorn 2006). Studies such as Bruneau et al. (2003), Cimellaro et al. (2006) and Bruneau and Reinhorn (2006) offer a definition of resilience to cover all actions that minimize losses from hazard, considering mitigation and recovery, making it possible to relate probability functions, fragilities, and resilience in a single integrated approach such that resilience can be quantified. Cimellaro et al. (2010) present these resilience concepts in a unified terminology for a common reference framework for quantification of disaster resilience by means of resilience functions, which provide a comprehensive understanding of damage, response, and recovery as they illustrate the time variation of damage as well as its relationship to response and recovery. Within this framework, a number of studies have explored the seismic resilience of different systems such as healthcare facilities (Bruneau and Reinhorn 2007), water resource systems (Wang and Blackmore 2009) or natural gas distribution networks (Cimellaro et al. 2014).

This study expresses results in terms of losses and downtime. Even though the approach followed in this work does not quantify resilience in absolute terms by means of a resilience function, it provides a process to reach initial targets of functionality valid in achieving a comprehensive resilience of structures (Bruneau and Reinhorn 2007). The results of this work provide key indicators that enable discussions with stakeholders in order to increase the resilience of existing buildings. This work demonstrates a relative increase in resilience from a baseline performance (archetype existing building) through adoption of a range of structural retrofits, non-structural enhancements and with mitigation measures which reduce or eliminate disruptions in presence of earthquake events.

Existing Tall Building Database

The SEAONC Committee on Performance Based Design of Tall Buildings developed a database of all buildings in San Francisco taller than 48.8 m (160 ft). The database tabulates building characteristics by location, height, number of stories, year built and lateral system type. Approximately 240 buildings greater than 48.8 m (160 ft) in height are identified. Fig 1a illustrates the number of tall buildings built each decade between 1900 and 2010. Interviews with practicing engineers and a partial database gathered previously by the SEAONC committee revealed information on the lateral system type for some of these buildings. Information on the remaining buildings was obtained by viewing construction documents available at the San Francisco Department of Building Inspection (DBI). The database identifies the lateral system type for approximately 80 out of the 240 buildings. The lateral system type of many buildings remains unknown because, while drawings of existing buildings are made available for viewing at the DBI (California Health and Safety Code 19850), access to drawings is limited by the difficulty in locating relevant structural information within the large microfilm archive.

In order to select a prototype building for this study, the data from the existing tall building database was disaggregated. Fig 1b shows the lateral system type for tall buildings built between 1960 and 1990. The sub-category 'Other System' means that the lateral system of the building is known and it is not a steel moment frame, while the sub-category 'Unknown System' is designated for all buildings for which the lateral system is unknown. This data reveals that the steel Moment Resisting Frame (MRF) system was the most prevalent type in pre-1990s construction for buildings greater than 35 stories in height. A sidewalk survey of a random sample of these tall buildings revealed that most are regular in plan, though some have setbacks up the height and others lack corner columns.

Archetype Building

A 40-story steel MRF was selected as a representative archetype tall building. The archetype building is regular in plan and represents the state of design and construction practice from the mid-1970s to the mid-1980s. Based on examination of existing building drawings, the archetype building layout consists of: 38 levels of office space; 2 levels for mechanical equipment (one at mid-height and one at the roof); 3 basement levels for parking; building enclosure composed of precast concrete panels and glass windows; floor system composed of concrete slab 76.2 mm (3 in) over metal deck 63.5 mm (2.5 in) supported by steel beams; columns of A572 (50 ksi) steel and beams of A36 (36 ksi). As illustrated in Fig 2, the prototype system consisted of a space frame with 6.1 to 12.2 m spans (20 to 40 ft) using wide flange beams, built up box columns and welded beam-column connections. Typical story heights are 3 m (10 ft) for basement levels, 6.1 m (20 ft) at ground level (lobby) and 3.8 m

(12.5 ft) for typical office levels. The overall height of the structure is 154.7 m (507.5 ft) above ground and 9 m (30 ft) below grade.

The design of the prototype building follows the provisions of the Uniform Building Code of 1973 (UBC 1973) and the 1973 Structural Engineers Association of California (SEAOC) Blue Book (SEAOC 1973), which was commonly employed to supplement minimum design requirements. Based on discussions with engineers whose firm designed such buildings (personal correspondence, H. J. Brunnier Associates), lateral wind forces generally governed the design of tall buildings over seismic forces in the 1973 UBC, and member sizes would have been sized for wind demand and detailed to provide a ductile response under seismic excitation. While the 1973 UBC does not specify drift limits, design offices would have implemented drift limits established by their firm's practice or those obtained from the SEAOC Blue Book of the time. For this study, the drift limit recommendations from Appendix D of the SEAOC Blue Book (1973) are used, equal to 0.0025 for wind and 0.005 for seismic for buildings taller than 13 stories. Current seismic drift limits are slightly more stringent: 0.020 times the story height, which for a deflection amplification factor of 5.5 as prescribed for special steel MRF, is approximately 0.004 (ASCE 2010). For the prototype building, since wind drift limits governed the MRF section sizes, beams and columns have low strength utilization ratios under code prescribed forces. The effective wind base shears with the forces prescribed by UBC 73 are 2.17% in the long direction of the building and 3.25% in the short direction, whereas the overall effective seismic base shear is 2.06%.

Typical member sizes and connection details were verified against available existing building drawings. Consistent with these records, built-up box columns and wide flange beams are selected for the prototype building. A summary of the design section sizes of the steel MRF are illustrated in Table 1. Fig 3 illustrates some of the typical details frequently observed in existing building drawings. Since the switch in the weld process that led to welds with very low toughness, as evidenced by fractures observed in the 1994 Northridge earthquake, took place in the mid-1960s (FEMA 2000), it is assumed that that fracture prone pre-Northridge moment connections are common. Designs of the 1970's did not include consideration of panel zone flexibility or strong column-weak beam principles. Krawinkler's panel zone model was not developed until 1978 (PEER 2010b) and strong column-weak beam requirements were not introduced in the UBC provisions until 1988 (SAC 2000). Column splices are typically located 1.2 m (4 ft) above the floor level approximately every three floors. Observed typical splice connection details consist of partial joint penetration welds of half the thickness of the smaller section being connected. When subject to tensile forces, these splices can only carry a fraction of the moment capacity and/or axial tension capacity of the smallest section size being connected. Furthermore, experimental tests on heavy steel section welded splices have illustrated sudden failures with limited ductility (Bruneau and Mahin 1990). Based on this evidence, column splice failures are considered in our assessment.

Analytical Model

The component models to represent non-linear columns, beams, panel zones and splices are described in this section. Concrete slabs are modeled as elastic cracked concrete 2D shell elements to represent the flexible floor diaphragm. Columns are modeled as lumped plasticity beam elements with yield surfaces capable of capturing interaction between bi-axial bending moment and axial force. Buckling in compression is also captured. Degradation parameters for response under cyclic loads are calibrated based on experimental tests of tubular steel columns (Kurata et al. 2005) following the guidelines for tubular hollow steel columns under varying levels of axial load (Lignos and Krawinkler 2010).

Beams that form part of the moment frames are modeled as lumped plasticity elements with implicit degradation in bending to capture random fracture at the connections. The random fracture model follows the methodology proposed by Maison and Bonowitz (1999), in which the plastic rotation at which fracture occurs is a random variable characterized by a truncated normal distribution following tests designed for typical pre-Northridge practice. Top and bottom capacities are modeled as a single random variable with a mean plastic rotation capacity of 0.006 radians and a standard deviation of 0.004 radians. The truncated tail at zero plastic rotation denotes fracture prior to yield, which is supported by data from the SAC studies (SAC 2000). When fracture prior to yield occurs, it is set at 70% of the moment capacity of the beam. The residual moment capacity after fracture is set at 25% of the beam capacity. For each of the analysis runs, subject to a unique earthquake record, a different random fracture sample is assigned for each of the moment connections in the building model. Therefore, all analysis runs for the archetype building model have a unique distribution of plastic rotation capacities throughout the structure. However, when assessing retrofit schemes, the distribution of plastic rotation capacities is consistent with the analysis runs from the baseline building model to enable a direct assessment of performance enhancement as a result of the retrofit measures adopted.

Panel zones are modeled using the Krawinkler model as outlined in PEER/ATC-72-1 (2010b) by the use of an assembly of rigid links and rotational springs that capture the tri-linear shear force-deformation relation. Since the prototype building model is three dimensional and columns are built-up box sections, the shear force-deformation relationship in each direction is assumed decoupled. Column splices are modeled as non-linear springs capable of reaching their nominal capacity with a sudden brittle failure followed by 20% residual capacity when subject to axial tension and/or bending. Full column capacity is assumed in compression since this is achieved by direct bearing.

Analytical models are subject to ground motions in conjunction with expected gravity loads associated with the seismic weight of the structure. Seismic weight includes self-weight, superimposed dead load and 25% of the unreduced live loads. 2.5% damping is assumed in the analysis (PEER 2010a). A fixed base is assumed at foundation level and soil-structure interaction is not considered. Ground Motions are input at top of foundation level.

Seismic Hazard and Ground Motions

The majority of tall buildings in San Francisco are clustered in the downtown area, located approximately 14 km from the San Andreas Fault and 16 km from the Hayward Fault. The authors conducted a site specific PSHA at a representative site, near the San Francisco Transbay Transit Center development, with subsurface ground conditions consistent with Site Class D (as defined in ASCE 7-10 2010) for the 10% in 50 year hazard. The selected intensity level is also representative of the "expected earthquake" defined by SPUR for the purpose of defining resilience. This "expected earthquake" corresponds to a 7.2 earthquake scenario, which is an event that can be expected conservatively, but reasonably within the lifetime of a structure (SPUR 2012). Reference to such scenario earthquake is important as it is a concept easier to grasp than probabilistic measures and therefore effective for communicating risk to policymakers and the public.

Forward directivity effects are known to cause pulselike ground motions at near-fault sites. Pulselike ground motions place extreme demands on structures and are known to have caused extensive damage in previous earthquakes (Shahi and Baker 2011). Due to the site's close proximity to active faults, near-fault directivity effects are expected to significantly contribute to the hazard. Therefore, a methodology proposed by Almufti et al. (2013), which is an extension of the method proposed by Shahi and Baker (2011), is utilized to incorporate velocity pulses in the selection of the design level ground motions for this study. This methodology uses disaggregation information from the PSHA to construct a suite of target spectra used for matching an appropriate proportion of pulselike motions with characteristics (pulse amplitude and pulse period) representative of a desired hazard intensity level. This methodology has been successfully implemented in the development of ground motions of a peer-reviewed high rise project in San Francisco (Almufti et al. 2013).

A Conditional Mean Spectrum (CMS) approach is used to characterize short and long-period ground motions separately (Baker 2011). Two suites of bedrock motions are developed to cover the entire period range of interest from $0.2T_1$ to $1.5T_1$ as defined in ASCE 7-10 (2010), where T_1 is the fundamental period of the structure. Each suite consists of 11 bidirectional motions each. The short-period suite covers the range of periods from 0.5 to 4 seconds and the long-period suite covers the range of periods from 4 to 10 seconds. The archetype building has a fundamental period of approximately 5 seconds and therefore the period range of interest from 1 to 7.5 seconds is bounded by the two suites of motions. A pulse-included PSHA at bedrock is conducted at two conditioning periods, 0.75 seconds and 7.5 seconds, which are selected to best facilitate covering the period range of interest accounting for potential elongation of the fundamental period due to non-linearity of the archetype building and the structural retrofit schemes considered. The disaggregation of the pulse-included PSHA at the two conditioning periods reveals that approximately 20% of the short-period ground motions (2 out of 11 ground motions) contributing to the hazard are pulselike while approximately 80% of long-period ground motions (8 out of 11 ground motions) contributing to the hazard are pulselike. Arup's in house software SISMIC (2012) is used to conduct the pulse-included PSHA.

For each pulselike motion, a unique pulse-included CMS is developed as the target spectrum for the pulse component of the ground motion using the method of Shahi and Baker (2011). For non-pulselike motions, seed ground motions are selected based on disaggregation results, linearly scaled to the target at the conditioning period, and then spectrally matched to the conventional CMS, developed using epsilon correlations by Baker and Jayaram (2008). Once the bedrock ground motions are developed, a non-linear site response analysis is conducted using LS-DYNA (2013) in order to characterize soil shaking and obtain input motions for the structural analysis. The soil profile and non-linear soil properties, which define the shear modulus reduction curves utilized in the site response, were obtained from soil testing at the representative site.

The maximum and minimum demand surface response spectra for each suite of motions are shown in Fig 4. ASCE 7-10 (2010) requires that for site-specific ground motions the design level response spectra is no less than 80% of the code prescribed design level spectrum. Fig 5 illustrates compliance with this criterion as the Envelope of the Mean of the Maximum Demand (EMMD) surface response spectra for the short and the long-period motions is no less than 80% of design level spectrum over the period range of interest of the structure (shaded in grey) from 1 to 7.5 seconds. In order to meet this requirement, the scale factors applied to the short and long-period suite of motions are 1.0 and 1.6 respectively. Fig 5 shows that the EMDD is close to the 475 year probabilistic estimate of the hazard. These ground motions are utilized to conduct an intensity based performance assessment of the archetype building. The pulse components of the pulselike ground motions are applied evenly to each of the principal directions of the building, i.e. out of 8 pulselike motions, 4 are oriented in one direction while the other 4 are oriented 90 degrees from that direction. For non-pulselike motions, the maximum demand orientation is random relative to the principal axes of the structure.

Building Performance Model

Communicating performance as the probable consequences in terms of direct economic losses to repair earthquake damage can influence decision making. Financial institutions use quantitative statements of probable building repair cost expressed as a percentage of building replacement value. The authors use this metric for our study, where the costs are expressed in present dollars. Losses are expressed as a percentage of repair cost, i.e. the cost required to restore a building to its pre-earthquake condition, over total building cost, i.e. the cost required to rebuild with a new structure of similar construction. In this study, total replacement cost includes replacement of basic building structure, exterior enclosure, MEP (mechanical, electrical and plumbing) infrastructure as well as all tenant improvements and contents. Demolition and site clearance are not included in the total replacement cost since the intent is to estimate the direct losses. Based on a class 5 rough order of magnitude cost estimate based on the Association for the Advancement of Cost Engineering (AACE), the most likely estimated cost for the archetype building in San Francisco in present dollars is $330 per square foot with an accuracy range of -5% to +30% .

The building performance model is defined for this study as a model to assess the probability of earthquake losses and downtime. The methodology followed for the loss and downtime assessment is outlined in Fig 6 and described in more detail below. Strategies for increased resilience are also presented. Lastly, modeling uncertainty, which is inherent to the loss and downtime assessment methodologies, is also discussed.

Loss Assessment Methodology

Engineering demand parameters, including maximum interstory drift ratios and peak floor accelerations are obtained from the NLRHA at every story in the building under consideration. Fig 7 illustrates the input demand parameters for the archetype building and each of the retrofit schemes obtained from the NLRHA results, which are well within the limits currently specified in building codes such ASCE 7-10 (2010). These parameters are used as input demands to the building performance model, which contains structural and non-structural components at each story level for all components in the building that are susceptible to earthquake damage. Structural component quantities are based on the structural design of the archetype building. Non-structural component quantities are estimated based on typical quantities found in buildings of similar occupancy by use of the Normative Quantity

Estimation Tool (FEMA 2012). Normative quantities are an estimate of the quantity of components and contents likely to be present in a building of a specific occupancy based on gross square footage. These quantities were developed based on a detailed analysis of approximately 3,000 buildings across typical occupancies (FEMA 2012). This study assumes estimates of quantities at the 50th percentile level. Where possible, these quantities were verified with registered engineers for the validity and relevance of the components to a tall building designed in the mid-1970s, and modified where discrepancies were identified.

Each one of these structural and non-structural building components has a component fragility function. A component fragility function is a statistical distribution that indicates the conditional probability of incurring damage at a given value of demand, which is typically assumed to be lognormal distribution. Component fragility functions contain unique fragilities for each possible damage state in the component. For instance, standard partition walls, designated in Table 2 by fragility C1011.001a, have 3 possible damage states (DS): DS1 consists on minor cracking of the wall board, DS2 consists on moderate cracking or crushing of the wall boards typically around corners and DS3 consists on significant cracking or crushing of the wall boards and buckling of studs (FEMA 2012). Each damage state has an associated consequence function, from which the repair cost and repair time associated with the level of damage in the component is estimated. The occurrence of damage states is predicted by individual demand parameters, as determined from the NLRHA. For each realization, fragility functions are used in conjunction with demand parameters to determine a damage state for each component. Consequence functions are then used to translate damage states into repair or replacement costs (FEMA 2012). The direct economic losses for each realization are estimated by conducting this calculation for every component at every story throughout the building. Table 2 summarizes components included in the standard building performance model, including fragility number, category, quantities, units, demand parameter

(DP), number of damage states (NDS), as well as median (M), dispersion (D), mean repair cost (MRC) and mean repair time (MRT) for the first damage state (DS1). For illustration, one sample non-structural component included in the enhanced building performance model is shown in parenthesis in Table 2 for each component category.

Downtime Assessment Methodology

While seismic loss estimates associated with direct economic losses enable discussions with building owners and investors about how individual retrofit interventions can move buildings in the direction of becoming more resilient, they do not provide a quantitative measure of resilience. In addition to direct economic losses, there is great vulnerability to indirect economic losses due to downtime, defined as the time required to achieve a recovery state after an earthquake. The Structural Engineers Association of Northern California (SEAONC) defines three recovery states: re-occupancy of the building, pre-earthquake functionality and full recovery (Bonowitz 2011). Re-occupancy occurs when the building is deemed safe enough to be used for shelter, though functionality may not be restored. Functional recovery occurs when the building regains its primary function, i.e. it is operational. Lastly, full recovery occurs when the building is restored to its pre-earthquake condition, it follows from functional recovery once additional repairs for aesthetic purposes have been completed.

The REDi guidelines provide a detailed downtime assessment methodology for individual buildings and identify the likely causes of downtime such that these can be mitigated to achieve a more resilient design. The methodology identifies the extent of damage and criticality of building components that may hinder achieving a recovery state through the introduction of repair classes. Repair classes are assigned to the each damage state for each building component. Repair classes dictate whether the damage in the component hinders building re-occupancy, functional recovery or full recovery. If the damage in any component hinders achieving a certain recovery state, the component needs to be repaired before such recovery state can be achieved. Once the components that need repairing in order to achieve a certain recovery state have been identified, the methodology includes delay estimates associated with impeding factors, defined as those factors which may impede the initiation of repairs. Impeding factors include post-earthquake inspection, engineering mobilization, contractor mobilization, financing, permitting and long-lead time components. Following an earthquake, a building owner is expected to submit an inspection request if the structural integrity of the building is in question. Furthermore, the jurisdiction, tenants or insurance companies may also request an inspection regardless of the extent of damage. Following post-earthquake inspection, as illustrated in Fig 6, there are three distinct sequences of delays due to impeding factors, the longest of which controls and is used in the downtime estimate. The first sequence of delays is related to engineering mobilization, review or re-design and permitting. This accounts for the time required to engage an engineer for structural assessment if there is structural damage to the building, perform relevant structural calculations, as well as re-design and issue drawings depending on the level of damage to the structure. The second sequence of delays concerns contractor mobilization. The time required to mobilize a contractor is dependent on a number of factors such as the severity of damage, bidding or building height among others. Furthermore, the mobilization of a contractor to conduct repair work on tall buildings is dependent on the availability of tower cranes. In addition to contractor mobilization, long lead components are a key consideration of downtime. These components are not readily available in normal circumstances or are custom made. The repair schedule can be significantly impacted by long lead components as these items cannot be replaced until they have arrived on site. The last sequence of delays is related to financing. The lack of financing to fund repair work can result in significant delays. If the losses associated with earthquake damage exceed the funds available to fund repair work, additional sources of funding need to be sought out. The delays associated with securing such funds are dependent on the method of financing e.g. private loan versus insurance.

Following any delays associated with impeding factors, repair work can commence. The REDi guidelines provide a logical approach for labor allocation and repair sequencing of structural and non-structural components on a floor per floor basis. The repair sequence defines the order in which repairs take place. As illustrated in Fig 6, structural repairs need to be conducted at any given floor before repairs to other building components at that level (or above) can commence. Non-structural repairs are divided into the following categories: egress (stairs and elevators), façade (exterior partitions and cladding), MEP and office fitouts (heating, ventilation and air conditioning -HVAC, partitions and ceiling tiles). Once structural repairs at any given floor are complete, repair of non-structural components can commence, in parallel, following a rational approach, e.g. repair of interior partition walls cannot commence until HVAC ducts have been repaired. Overall repair time is estimated based the repair times dictated by PACT, which are expressed in number of days for a single worker to complete the work and the labor allocation for each floor in the building. Table 3 illustrates the labor allocation parameters employed in the repair work estimates. To account for subcontractor resource limitations, the number of workers repairing a certain type of component is limited. Such limit is also included in Table 3. Furthermore, the total number of workers in the building is also limited by the number of workers allocated to a project. Following discussions with contractors and cost estimators, the REDi guidelines define the total number of workers on the project as a function of the square footage of the building, which for the archetype building in this study corresponds to 114 workers. Work across multiple floors can take place simultaneously as long as the above constraints are met.

Lastly, utility disruption is also considered when estimating downtime for functional recovery. Disruption to water, natural gas and electrical systems is considered. The time required for achieving a 50% recovery of the system is assumed as 21, 42 and 3 days for water, natural gas and electrical systems respectively. Acknowledging the difficulty in performing accurate predictions of utility disruption, the REDi guidelines present a best estimate of recovery based on an assessment of performance of these systems in past earthquakes. In the present study, utility disruption does not control over other impeding factors in the overall downtime assessment and therefore do not have a direct impact on the downtime estimates. Equation 1 illustrates the overall downtime calculation by subdividing delays into the following categories: utility disruption, impeding factors and repair work.

$$\text{Downtime} = \text{MAX}\,(\text{Utility Disruption}^{*}, \text{Impeding Factor Delays}) + \text{Repair Work}^{**} \quad \textbf{(1)}$$

* For Full recovery and Functional Recovery only

** Including delays associated with long-lead time components

Strategies for Increased Resilience

In order enhance the seismic performance of the archetype building, a reduction in transient and residual deformations is required. This objective can be achieved by adding stiffness, damping or a combination of these to the structure. Two conceptual structural retrofit schemes are considered. The first scheme consists in the introduction of an elastic spine with steel bracing in the building core. The introduction of an elastic spine is intended to reduce transient and residual interstory drifts up the building height. This concept has been implemented in a number of retrofit projects in Japan and has been explored in studies such as Günay et al. (2009) by means of introducing a rocking wall. A second retrofit scheme consists in the introduction of base isolation at ground level and is intended to significantly reduce the seismic demands to the structure. This technique has been implemented in a number of retrofit projects in Japan (Kani and Katsuta 2009).

In addition to structural retrofit strategies, schemes for enhanced non-structural performance are also adopted in this study. These consist on employing non-structural components that are more resilient to earthquake damage. For instance, the component fragility function for standard partition walls is designated in Table 2 by fragility C1011.001a, which has a median value of 0.2% interstory drift ratio for DS 1. The component fragility for the enhanced partition wall is designated by fragility C101.001d, which has a median value of 1.7% interstory drift ratio for DS 1. This illustrates that enhanced non-structural components can withstand significantly larger deformations before reaching the same damage state. These differences result in less damage to the components in the enhanced building performance model versus those in the standard building performance model for the same demand parameter. In the case of the partition walls, where standard components are characterized by little deformation capacity and undergo damage at low drift ratios, enhanced partition walls can enable a shift of up to 1.5% drift before the initiation of damage. This is achieved through a simple sliding/frictional connection detail which isolates the partition from lateral deformations while at the same time providing some resistance to in-plane and out-of-plane inertia forces as described in Araya-Letelier and Miranda (2012). The impact of using enhanced non-structural components is evaluated in all three structural schemes considered. When baseline non-structural components are used, these are referred to as standard non-structural components. When non-structural components that are more resilient to earthquake damage are used, there are referred to as enhanced non-structural components.

In order to minimize downtime, a number of mitigation measures can be adopted. As illustrated in Equation 1, downtime to achieve re-occupancy is attributed to impeding factors and the time required to repair damaged structural and non-structural components. Downtime to achieve functional recovery is attributed to these same factors, but additionally considers utility disruption. The mitigation measures considered in this study in order to minimize delays associated with impeding factors are illustrated in Table 4. For instance, delays associated with post-earthquake inspection can be minimized by joining the City and County of San Francisco's Building Occupancy Resumption Program (BORP) to pre-certify a private post-earthquake inspection rather than waiting for a city appointed inspector. Similarly, delays associated with engineering and contractor mobilization can be minimized by arranging contractual agreements with engineers and contractors to guarantee their services immediately after an earthquake. For instance, as illustrated in Table 4, if damage to structural components hinders re-occupancy, expected delays associated with engineering mobilization are 12 weeks. However, these delays can be reduced down to 4 weeks by having an engineer on contract. Similarly, for the same level of structural damage, expected delays associated with contractor mobilization are 40 weeks, but these can be reduced to 7 weeks by having a pre-arranged contract with a general contractor. Similar measures can be put in place to minimize other impeding factors.

Modeling Uncertainty

Since there are many factors that can affect performance, such as intensity of ground shaking, building construction quality, building response or vulnerability of contents among others, there is significant uncertainty in the predicted performance of the building. However, losses can be expressed as a performance function, i.e. probability of losses of a specified amount or smaller incurred as a result of an earthquake. This uncertainty can be accounted by means of Monte Carlo simulation, where each realization represents one possible performance outcome for the building considering a single combination of possible values of each variable considered. The authors used PACT (FEMA 2012), which utilizes this methodology, for conducting the loss estimates for the archetype building and five schemes for enhanced performance including structural only enhancements, non-structural only enhancements and a combination of these. Each building performance assessment consists of 1000 realizations.

Structural modeling uncertainty results from inaccuracies in component modeling, damping and mass assumptions. These uncertainties are associated with the level of building definition, as well as the quality and completeness of the analytical model (FEMA 2012). Within PACT, these uncertainties are accounted for by defining a value of dispersion to the building definition and a value of dispersion to the analytical model. These values of dispersion are defined as superior, average or limited to reflect the overall modeling uncertainty. Since documents defining the building design were confirmed by visual observation, the authors selected average values of dispersion for construction quality assurance (FEMA 2012). Similarly, since the model contained most elements that contribute to the strength and stiffness as well as robust non-linear components over the range of the deformation response, the authors selected average values of dispersion for the quality of the analytical model. These values of dispersion are used to amplify the dispersion in the structural demand parameters, as illustrated in Figure 7, which are used as input to the PACT analysis.

Residual drifts are an important consideration when estimating losses. Typical building repair fragility as a function of residual drifts is a lognormal distribution with a median value of 1% residual drift ratio and a dispersion of 0.3. Residual drifts predicted by non-linear analysis are highly sensitive to component modeling assumptions (FEMA 2012). Accurate statistical simulation of residual drift requires the use of advanced component models, careful attention to cyclic hysteretic response, and a large number of ground motion pairs. Therefore, residual drifts were estimated as a function of peak transient response of the structure and the median story drift ratio calculated at yield based on FEMA P-58 (2012) recommendations. For each realization, PACT uses the maximum residual story drift together with the building repair fragility to determine if the building is deemed irreparable. If irreparable, repair cost and repair time are taken as the building replacement values. In order to assess the impact of residual drifts in the loss assessments, results were calculated with and without consideration of residual drifts.

Loss and Downtime Assessment

As illustrated in Table 5, expected losses for the archetype building are in the order of \$46M (34% of building cost). These losses are associated with the structural response demand parameters illustrated in Fig 7a. A structural only retrofit scheme, which consists of the introduction of an elastic spine with steel bracing in the building core, enables a reduction in expected losses by roughly 25% to \$34M (25% of building cost). The structural response demand parameters associated with this retrofit scheme are illustrated in Fig 7b. An alternate structural only retrofit scheme, which consists of the introduction base isolation at ground level, enables a reduction in expected losses by roughly 80%, to \$9M (7% of building cost). The structural response demand parameters associated with this retrofit scheme are illustrated in Fig 7c. A non-structural only scheme, which consists of the introduction of components that are more resilient to earthquake damage, enables a reduction in expected losses by roughly 32%, to \$31M (23% of building cost). When these non-structural enhancements are used in conjunction with the elastic spine structural retrofit scheme, a 56% reduction in expected losses, to \$20M (15% of building cost) is attained. Lastly, when these non-structural enhancements are used in conjunction with the base isolation structural retrofit scheme, a 92% reduction in expected losses, to \$4M (3% of building cost) is achieved. These results explicitly consider the impact of residual drifts. If the impact of residual drifts is neglected, a reduction in expected losses is observed as illustrated in Table 5. These results can also be visualized in Fig 8 by fitting all 1,000 realizations in each performance assessment to a lognormal distribution. Since the engineering demand parameters used as input to the building performance model are in line with current code requirements, it is no surprise that expected losses in new tall buildings are not drastically different than those of older tall buildings. The expected losses for an archetype 40 story building in the Los Angeles area designed per current buildings codes under an equivalent intensity level are 23% of building cost (Shome et al. 2013).

Fig 9 illustrates the contribution of different building components to the total expected losses. Building components are grouped into five main categories: egress, façade, MEP, office fitouts and structure. The performance groups associated with each one of these categories is shown in Tables 2. There are similarities in the distribution of building components contributing to the losses between the archetype building and the elastic spine structural retrofit scheme with either standard or resilient structural components. This can be attributed to the similarity in the demand parameter distribution throughout the height for both schemes, as shown in Fig 7. The distribution of building components contributing to the losses for the base isolated scheme is distinct due to the unique distribution in demand parameters throughout the building height when compared to the other structural schemes. The use of resilient non-structural building components enables a significant reduction in losses attributed to damage to the façade (up to 93% for the elastic spine scheme), office fitouts (up to 94% for the base isolated scheme) and MEP components (up to 97% for the base isolated scheme). Structural losses are largely due to damage to fracture prone pre-Northridge moment connections (70% to 90% depending on the structural scheme). However, these losses vary in absolute value from $5M for the archetype building to $2M for the base isolated scheme. Absolute losses attributed to egress are a result of direct damage to elevators, which require repair costs ranging from $9M for the archetype building to $0.5M for the base isolated scheme.

The discrepancies in the results with and without consideration of residual drifts can be observed in Fig 8 by the dispersion of the lognormal distributions. For the archetype building with standard non-structural components, the dispersion is 0.44 when residual drifts are neglected and 0.61 when residual drifts are considered. Similarly, for the elastic spine scheme with standard non-structural components, the dispersion has a value of 0.51 when residual drifts are neglected and 0.64 when considered. This increase in the dispersion is smaller than that of the archetype building. Lastly, for the base isolated case, the dispersion remains effectively constant at approximately 0.86. A similar trend is observed for the schemes considered when enhanced non-structural components are used. These observations highlight how as the schemes considered become more resilient, there is less variability throughout the set of realizations. Even though consideration of residual drifts increase the dispersion in the building performance functions, as illustrated in Fig 8, their consideration is critical in the loss estimate methodology since a building may be deemed irreparable if large residual drifts are present. Furthermore, residual drifts are an important consideration in judging the post-earthquake safety of a building. Field manuals for post-earthquake safety evaluation, such as ATC 20-1 (2005), indicate that when any story in a building has noticeable leaning the building should be posted with an 'Unsafe' placard, which categorizes the building as unsafe for occupancy or entry. The REDi downtime assessment methodology assumes that residual drifts are small and therefore the building is repairable. Consideration of residual drifts on the downtime estimate results presented in Table 6 would increase expected values because for large residual drifts, where the building is deemed unrepairable, total downtime is that of complete re-design and re-construction. FEMA P-58 (2012) proposes 4 damage states associated with residual drift: Damage State 1 (DS1) requires no structural realignment, though repairs may be required for non-structural components; Damage State 2 (DS2) requires realignment of the structural frame and related structural repairs; Damage State 3 (DS3) requires major structural realignment to restore margin of safety for lateral stability though the level of repair may not be economically feasible; lastly, Damage State 4 (DS4) implies that the structure is in danger of collapse from aftershocks. Fig 10 illustrates probability distribution of residual drifts for the baseline building, elastic spine and base isolated retrofit schemes against the abovementioned damage states. The expected residual drift for the baseline building is 0.44%, consistent with DS2. The expected residual drift for the elastic spine retrofit scheme is 0.23%, just beyond the threshold of DS1. The expected residual drifts for the base isolated scheme is 0.07%, consistent with DS1 and well below the maximum out-of-plumb tolerance permitted in new construction.

In order to provide a more direct measure of resilience, the downtime to achieve building re-occupancy and functional recovery for the archetype building and retrofit schemes considered is presented in Table 6. These results illustrate that while structural retrofits may enable significant reductions in losses, as seen in Table 5, these measures alone do not ensure a building is resilient. An illustration of the impact of using enhanced non-structural components as well as mitigation measures to minimize delays associated with impeding factors is illustrated in Fig 11, where a breakdown of the different downtime contributors as well as disaggregation of the impeding factors for the archetype building is shown. For the same structural scheme, it can be observed that using enhanced non-structural components and adopting mitigation measures can have a significant impact on downtime. Downtime for re-occupancy for all structural schemes with standard non-structural components is largely driven by delays associated with building inspection, contractor mobilization and long leads components that require replacement. In addition to these delays, which are equal for all schemes, repair times range from 32 weeks for the baseline and elastic spine schemes down to 12 weeks for the base isolation scheme. Downtime for functional recovery for structural schemes with standard non-structural components vary: 87, 72 and 59 weeks for the baseline, elastic spine and base isolation schemes respectively. Utility disruption does not control overall downtime estimates for functional recovery because delays associated with impeding factors exceed those associated with utility disruption (see Equation 1). While delays are consistent with those for re-occupancy, repair times are as follows: 46, 31 and 18 weeks for the baseline, elastic spine and base isolation schemes respectively. Repair times for re-occupancy are consistent between the baseline scheme and the elastic spine because, while the elastic spine scheme reduces damage and losses to certain components, it does not prevent damage to those components that hinder re-occupancy. However, repair times for functional recovery for the elastic spine scheme are significantly lower than for the baseline scheme because lower residual drifts reduce damage to elevators. When enhanced non-structural components are adopted in addition to measures to mitigate delays, downtime for re-occupancy can be drastically reduced to 14 weeks for the baseline and elastic spine schemes and a day or less for the base isolated scheme. Furthermore, downtime for functional recovery can be reduced to 32 weeks for the baseline case, 20 weeks for the elastic spine scheme and a day or less for the base isolation scheme.

As discussed earlier, there is a great deal of uncertainty in the prediction of losses and downtime associated with the seismic performance of the building. In addition to the high level of uncertainty, there are also a number of limitations associated with this work relating to the development of the archetype building, the analytical model of the structure and the building performance model. Even though the development of the archetype building is based on an existing tall building database, a review of existing building drawings and discussions with practicing engineers of the time, access to this data was limited and therefore the archetype building is not representative of the entire existing tall building stock. Additionally, while the analytical model attempts to account for all sources of strength and stiffness contribution to the seismic response of the structure, additional studies (large number of analyses with varying modeling assumptions) are required to assess the sensitivity of modeling parameters in the overall structural response. As earlier explained, the variability in structural response is incorporated into the loss estimation methodology though a modeling dispersion. Limitations to the building performance model result from building component quantity estimates, component fragility functions and the downtime estimate methodology. Structural and non-structural quantity estimates are based on the Normative Quantity Estimation Tool (FEMA 2012) as opposed to specific inventories of the existing tall buildings that are representative of the archetype building. Component fragility functions (fragility and consequence data) were not explicitly developed for the different building components, but rather adopted from a fragility database developed as part of FEMA P-58 (2012) project. Lastly, downtime estimates are developed based on the REDi guidelines. Accurate predictions of downtime are difficult to achieve due to the large uncertainty and factors involved. However, the methodology follows a rational approach and enables a best estimate of disruption to achieve certain recovery states after an earthquake. A more complete evaluation should also consider performance under various hazard levels, recognizing that the design level earthquake is simply an index to evaluate overall risk. Evaluation of a wider range of intensities (return periods) would establish whether the performance expressed in terms of losses and downtime at a design level earthquake is a realistic and reliable basis for making decisions and would enable conducting a cost-benefit analysis of the different schemes considered.

Summary and Conclusions

A seismic performance assessment of existing tall steel-framed buildings has been presented for a case study city, San Francisco, where an archetype tall building is designed based on an inventory of the existing tall building stock. In order to influence decision making, performance is reported as the expected consequences in terms of direct economic losses and downtime. A number of strategies including structural retrofits, non-structural enhancements and mitigation measures are proposed in order to achieve increased resilience. Expected direct economic losses for the archetype building are in the order of 34% of building cost and the adoption of structural retrofit schemes, enhanced non-structural components and mitigation measures to minimize impeding factors enable up to a 92% reduction in losses. The adoption of non-structural enhancements can enable significant reduction in losses associated with the performance of the façade, office fitouts and MEP components, though overall loss reduction is maximized when adopting both structural and non-structural enhancements. Downtime for re-occupancy and functional recovery of the archetype building is estimated at 71 weeks and 87 weeks respectively. When mitigation measures to reduce delays are used in conjunction with both structural and non-structural enhancements, minimal downtime for both re-occupancy and functional recovery can be achieved. The impact of residual drifts in seismic loss estimates for the archetype building and retrofit schemes under consideration is quantified. Consideration of residual drifts in the loss assessment yields an increase in expected losses as well as an increase in the dispersions of the resulting performance functions. Furthermore, building performance is categorized as a function expected residual drifts, which indicates that the archetype building requires structural realignment of the frame under a design level earthquake, whereas the retrofit schemes presented reduce damage to levels requiring very minor or no structural realignment.

Future work should consider the development of additional archetype buildings that enable representation of a larger proportion of the building stock. Additionally, time based assessments in conjunction with cost benefit analyses of the different enhancement schemes should be studied in order to incentivize the adoption of these retrofit measures. The results of these studies should target building owners and policy makers, who can adopt measures to ensure that the resilience of existing tall buildings enables a successful recovery following a major earthquake.

Tables

Table 1. Lateral resisting system section sizes per the 1973 UBC design.

Level Range	Wide Flange Beams			Box Columns		
	Exterior Short Span	Interior Short Span	Interior Long Span	Interior	Ext. Short EL. (x)	Ext. Long EL. (y)
Base to 10	W36x256	W36x282	W30x124	22x22” t=3”	26x26” t=3”	20x20” t=2.5”
11 to 20	W33x169	W36x194	W27x84	20x20” t=2”	26x26” t=2.5”	20x20” t=2”
21 to 30	W33x118	W33x169	W27x84	18x18” t=1”	24x24” t=1.5”	18x18” t=1”
30 to Roof	W24x62	W27x84	W24x76	18x18” t=0.75”	24x24” t=3”	18x18” t=0.75”

Table 2. Fragility numbers, category, quantities, units, demand parameter (DP), number of damage states (NDS), median (M), dispersion (D), mean repair cost (MRC) and mean repair time (MRT) for the first damage state (DS1) of each component in the standard building performance model.

						DS1			
Fragility Number	Category	Quantity	Unit	DP	NDS	M	D	MRC	MRT (days)
B1031.001	Structure	3096	1 EA	IDR	3	0.040	0.40	$12,107	34.66
B1031.011c	Structure	26	1 EA	IDR	3	0.040	0.40	$21,363	58.64
B1031.021b	Structure	112	1 EA	IDR	3	0.040	0.40	$10,246	30.13
B1031.021c	Structure	226	1 EA	IDR	3	0.040	0.40	$11,446	33.66
B1035.041	Structure	456	1 EA	IDR	5	0.017	0.40	$11,980	31.95
B1035.042	Structure	318	1 EA	IDR	5	0.017	0.40	$12,313	34.77
B1035.051	Structure	1552	1 EA	IDR	5	0.017	0.40	$16,653	45.71
B1035.052	Structure	856	1 EA	IDR	5	0.017	0.40	$16,653	44.41
B2011.201a (B2022.202)	Façade	533 (6933)	390 SF (30 SF)	IDR	2	0.005 (0.020)	0.50 (0.30)	$17,160 ($1,320)	184.60 (1.00)
C1011.001a (C1011.001d)	Fitout	365	100 LF	IDR	3	0.002 (0.017)	0.60	$2,733	8.04 (1.61)
C3011.001a	Fitout	28	100 LF	IDR	1	0.002	0.60	$2,829	9.00
C3027.001	Fitout	2736	100 SF	A	1	0.500	0.50	$121	0.43
C3032.001b	Fitout	547	600 SF	A	3	0.550	0.40	$921	3.03
C3034.001	Fitout	6192	1 EA	A	1	0.600	0.40	$483	1.51
E2022.023	Fitout	2554	1 EA	A	1	0.400	0.50	$1,000	0.00
D2021.011a (D2021.014a)	MEP	6	1000 LF	A	2	1.500 (2.250)	0.40 (0.50)	$348	1.02
D2022.011a	MEP	37	1000 LF	A	2	0.550	0.50	$279	1.00
D2022.011b	MEP	37	1000 LF	A	2	1.200	0.50	$383	1.00
D2022.021a	MEP	14	1000 LF	A	2	1.500	0.50	$348	1.00
D2031.021a	MEP	24	1000 LF	A	1	2.250	0.50	$3,167	9.31
D2031.021b	MEP	24	1000 LF	A	2	1.200	0.50	$423	1.25
D3041.011a	MEP	31	1000 LF	A	2	1.500	0.40	$681	2.00
D3041.012a	MEP	8	1000 LF	A	2	1.500	0.40	$996	2.29
D3041.031a	MEP	372	10 EA	A	1	1.300	0.40	$2,833	10.00
D3041.041a	MEP	289	10 EA	A	1	1.900	0.40	$14,796	41.49
D4011.021a	MEP	83	1000 LF	A	2	1.100	0.40	$348	1.05
D4011.031a	MEP	37	100 EA	A	2	0.750	0.40	$526	1.25
D5012.021a	MEP	43	1 EA	A	1	1.280	0.40	$9,707	9.25
D3031.011c	MEP	2	500 TN	A	1	0.200	0.40	$263,967	248.19
D3031.021c	MEP	2	500 TN	A	1	0.500	0.40	$134,657	126.74
D3052.011d	MEP	13	30000 CF	A	2	0.250	0.40	$2,066	6.48
D5012.013a	MEP	17	1 EA	A	1	0.730	0.45	$4,167	10.62
C2011.001b (C2011.001a)	Egress	43	1 EA	IDR	3	0.005 (0.010)	0.60	$394	1.08
D1014.011	Egress	12	1 EA	A	4	0.390	0.45	$1,333	3.90
D1014.014	Egress	12	1 EA	Res-IDR	1	0.002	0.30	$1,200,000	180.00

Table 3. Labor allocation parameters for repair time estimates. Adapted from REDi.

Component Category	Number of Workers	Maximum Number of Workers
Structure	1 per 500 ft^2	20
Façade	1 per 1000 ft^2	45
Office Fitouts	1 per 1000 ft^2	45
Egress	2 per Damaged Unit	27
MEP	3 per Damaged Unit	18

Table 4. Mitigation measures to minimize delays associated with impeding factors. Adapted from REDi.

Impeding Factor	Mitigation Measure	Other Conditions	Mean	Dispersion
Post-Earthquake Inspection	None	-	5 days	0.54
	BORP Program	-	1 day	0.54
Engineering Mobilization	None	Damage to structural components does not hinder Full Recovery	6 weeks	0.40
		Damage to structural components hinders Re-ocuppancy	12 weeks	0.40
		Complete re-design required	50 weeks	0.30
	Engineer on Contract	Damage to structural components does not hinder Full Recovery	2 weeks	0.30
		Damage to structural components hinders Re-ocuppancy	4 weeks	0.50
		Complete re-design required	42 weeks	0.50
Contractor Mobilization	None	Damage to structural components does not hinder Full Recovery	28 weeks	0.30
		Damage to structural components hinders Re-ocuppancy	40 weeks	0.30
	General Contractor on Contract	Damage to structural components does not hinder Full Recovery	3 weeks	0.70
		Damage to structural components hinders Re-ocuppancy	7 weeks	0.40
Financing	None	Private Loans	15 weeks	0.70
	Pre-arranged Credit	-	1 week	0.50
Permitting	None	Damage to structural components does not hinder Full Recovery	1 week	0.90
	Minimize Structural Damage	Damage to structural components hinders Re-ocuppancy	8 weeks	0.30

Table 5. Expected loss estimates for the baseline building and enhanced performance schemes with and without consideration of residual drifts.

Residual Drift Considered		Non-structural Standard	Non-structural Enhanced	Residual Drift Neglected		Non-structural Standard	Non-structural Enhanced
Structural	Archetype (Baseline)	$46M (34%)	$31M (23%)	Structural	Archetype (Baseline)	$35M (25%)	$19M (14%)
	Elastic Spine	$34M (25%)	$20M (15%)		Elastic Spine	$29M (21%)	$13M (10%)
	Base Isolation	$9M (7%)	$4M (3%)		Base Isolation	$9M (7%)	$4M (3%)

Table 6. Downtime estimates for the baseline building and enhanced performance schemes for re-occupancy and functional recovery.

Re-occupancy		Non-structural Standard	Non-structural Enhanced	Functional Recovery		Non-structural Standard	Non-structural Enhanced
Structural	Archetype (Baseline)	72 weeks	14 weeks	Structural	Archetype (Baseline)	87 weeks	32 weeks
	Elastic Spine	72 weeks	14 weeks		Elastic Spine	72 weeks	20 weeks
	Base Isolation	53 weeks	1 day		Base Isolation	59 weeks	1 day

Acknowledgments

The authors would like to acknowledge the SEAONC Tall Buildings Committee for their effort in developing the existing tall building database for San Francisco. We would like to thank Jack Baker and Jongwon Lee for their guidance in the seismic hazard and ground motion selection work. We would like to thank Sean Merrifield and Jenni Tipler for their support in the development of the PACT analysis model and Eduardo Miranda for his guidance on the overall loss assessment, particualy with regards to residual drift considerations. We would like to thank Laurence Kornfield for proving insight on how to maximize the impact of this work on future policy in San Francisco. We would also like to thank Arup for providing research funds to conduct this work. Lastly, we would also like to thank Tiziana Rossetto for enabling Carlos Molina Hutt to temporarily relocate to San Francisco to work on this research.

References

Almufti, I., Motamed , R., Grant, D. and Willford, M. (2013). "Incorporation of velocity pulses in design ground motions for response history analysis using a probabilistic framework." *Earthquake Spectra*, accepted.

Almufti, I. and Willford, M. (2013). "Resilience-based Earthquake Design Initiative (REDi) for the Next Generation of Buildings." Arup, <http://publications.arup.com/Publications/R/REDi_Rating_System.aspx> (Sept. 1, 2014).

Araya-Letelier, G. and Miranda E. (2012). "Novel Sliding/Frictional Connections for Improved Seismic Performance of Gypsum Wallboard Partitions." *Proc., 15th World Conference of Earthquake Engineering*, Lisbon, Portugal.

ASCE (2010). "Minimum design loads for buildings and other structures." ASCE/SEI 7-10, American Society of Civil Engineers, Reston, VA.

ATC (2005). "Field manual: postearthquake safety evaluation of buildings (second edition)". ATC-20-1, Applied Technology Council, Redwood City, California.

Baker, J. (2011). "Conditional Mean Spectrum: Tool for ground motion selection." *Journal of Structural Engineering*, 137(3), 322–331

Baker, J. and Jayaram, N. (2008). "Correlations of spectral acceleration values from NGA ground motion models." *Earthquake Spectra,* 23(1), 299-317.

Bonowitz, D. (2011). "Resilience Criteria for Seismic Evaluation of Existing Buildings." A 2008 Special Projects Initiative Report to Structural Engineers Association of Northern California, San Francisco, California.

Bruneau, M., Chang, S., Eguchi, T., Lee, G., O'Rourke, T., Reinhorn, A., Shinozuka, M., Tierney, K., Wallace, W. and Winterfeldt, D. (2003). "A Framework to Quantitatively Assess and Enhance the Seismic Resilience of Communities." *Earthquake Spectra*, 19(4). 733–752.

Bruneau, M. and Mahin, S. (1990). "Ultimate behavior of heavy steel section welded splices and design implications." *Journal of Structural Engineering*, 116(8).

Bruneau, M. and Reinhorn, A. M. (2006). "Overview of the Resilience Concept." *Proc., 8th U.S. National Conference on Earthquake Engineering*, San Francisco, CA.

Bruneau, M. and Reinhorn, A. M. (2007). "Exploring the concept of seismic resilience for acute care facilities." *Earthquake Spectra*, 23(1), 41-62.

CERC (2012). "Christchurch, the city and approach to this inquiry." Canterbury Earthquakes Royal Commission, Final Report, Volume 5, Canterbury, New Zealand.

Cimellaro, G. P., Reinhorn, A. M. and Bruneau, M. (2006). "Quantification of Seismic Resilience." *Proc., 8th U.S. National Conference on Earthquake Engineering*, San Francisco, CA.

Cimellaro, G. P., Reinhorn, A. M. and Bruneau, M. (2010). "Framework for analytical quantification of disaster resilience." Engineering Structures, 32 (2010) 3639-3649.

Cimellaro, G. P., Villa, O. and Bruneau, M. (2014). "Resilience-Based Design of Natural Gas Distribution Networks." *ASCE Journal of Infrastructure Systems*, 05014005(14).

Comerio, M. (2006). "Estimating Downtime in Loss Modeling." *Earthquake Spectra,* 22(2), 349-365.

FEMA (2000). "Recommended postearthquake evaluation and repair criteria for welded steel moment-frame buildings. Program to reduce the hazards of steel moment frame structures." FEMA 352, Federal Emergency Management Agency, Washington, D.C.

FEMA (2006). "Next generation performance based seismic design guidelines. Program plan for new and existing buildings." FEMA 445, Prepared by the Applied Technology Council for the Federal Emergency Management Agency, Washington, D.C.

FEMA (2012). "Seismic performance assessment of buildings." FEMA P-58, Prepared by the Applied Technology Council for the Federal Emergency Management Agency, Washington, D.C.

Günay S., Korolyk M., Mar D., Mosalam K.M. and Rodgers J. (2009). "Infill walls as a spine to enhance the seismic performance of non-ductile reinforced concrete frames." *Proc., Applied Technology Council and the Structural Engineering Institute 2009 Conference on Improving the Seismic, Performance of Existing Buildings and Other Structures*, San Francisco, CA.

Gupta A. and Krawinkler H. (1999). "Seismic Demands for Performance Evaluation of Steel Moment Resisting Frame Structures." Dept. of Civil and Environmental Engineering, Stanford University. Report No. 132, Stanford, California.

IBC (2012). "2012 International Building Code." IBC 2012, International Code Council, INC.

Jayaram, N. and Shome N. (2012). "A Statistital Analysis of the Response of Tall Buildings to Recorded and Simulated Ground Motions." *Proc., 15th World Conference of Earthquake Engineering*, Lisbon, Portugal.

Kani, N. and Katsuta, S. (2009). "Seismic Isolation Retrofit for Existing Buildings in Japan." *Proc., Applied Technology Council and the Structural Engineering Institute 2009 Conference on Improving the Seismic, Performance of Existing Buildings and Other Structures*, San Francisco, CA.

Khater, M., Scawthron, C. and Johnson, J. (2002). "Loss Estimation." *Earthquake Engineering Handbook,* Chapter 31, CRC Press, Boca Raton, Florida, USA.

Krawinkler, H. and Miranda, E. (2004). Performance-Based Earthquake Engineering. In: Bozorgnia Y. and Bertero V., *Earthquake Engineering: From Engineering Seismology to Performance-Based Engineering*, CRC Press, Chapter 9.

Kurata, M., Suita, K. and Nakashima, M. (2005). "Test on large cyclic deformation of steel tube columns having fixed column bases.", *Journal of Structural and Construction Engineering*, 598,149-154.

Lignos, D. and Krawinkler, H. (2010). "A steel database for component deteriorration of tubular hollow square steel columns under varying axial load for collapse assessment of steel structures under earthquakes". *Joint Conference Proceedings: 7th Internation Conference on Urban Earthquake Engineering & 5th International Conference on Earthquake Engineering*, Tokyo Institute of Technology, Tokyo, Japan.

LS-DYNA (2013). Livermore Software Technology Corporation (LSTC) Version 971.

Maison, F. and Bonowitz, D. (1999). "How safe are pre-Northridge WSMFs? A case study of the SAC Los Angeles nine-story building." *Earthquake Spectra,* 15(4).

Miranda, E. and Aslani, H. (2003). "Probabilistic Response Assessment for Building-Specific Loss Estimation." Pacific Earthquake Engineering Research Center, Report No. 2003/03, College of Engineering, University of California, Berkeley.

Moehle, J. and Deierlein, G. (2004). "A framework methodology for performance-based earthquake engineering." *Proc., 13th World Conference of Earthquake Engineering*, Vancouver, B.C., Canada

Muto, M. and Krishnan, S. (2011). "Hope for the Best, Prepare for the Worst: Response of Tall Steel Buildings to the ShakeOut Scenario Earthquake." *Earthquake Spectra*, 27(2).

PEER (2010a). "Tall buildings initiative: guidelines for performance-based seismic design of tall buildings." Pacific Earthquake Engineering Research Center, Report No. 2010/05, College of Engineering, University of California, Berkeley.

PEER (2010b). "Modeling and acceptance criteria for seismic design and analysis of tall buildings." Pacific Earthquake Engineering Research Center, Report No. 2010/111 also published as PEER/ATC-72-1, College of Engineering, University of California, Berkeley, CA.

Porter, K. and Kiremidjian, A .S. (2001). "Assembly-Based Vulnerability of Buildings and Its Uses in Seismic Performance Evaluation and Risk Management Decision-Making" Dept. of Civil and Environmental Engineering, Stanford University. Report No. 139, Stanford, California.

SAC (2000). "Performance prediction and evaluation of steel special moment frames for seismic loads." SAC Steel Project, Report No. SAC/BD-00/25, Richmond, CA.

SEAOC (1973) "Recommended lateral force requirements and commentary." Seismology Committee, Structural Engineers Association of California, Sacramento, CA.

Shahi, S. K. and Baker, J.W. (2011). "An empirically calibrated framework for including the effects of near-fault directivity in probabilistic seismic hazard analysis." *Bulletin of the Seismological Society of America*, 101(2), 742–755.

Shome N., Jayaram, N. and Rahnama, M. (2013). "Development of Earthquake Vulnerability Functions for Tall Buildings." *Proc., 11th International Conference on Structural Safety and Reliability*, New York, USA.

SISMIC (2012). Oasys Sismic: Probabilistic Seismic Hazard Program, Version 9.2.0.10b, Arup.

SPUR (2012). "Safe Enough to Stay." San Francisco Planning and Urban Research Association, <http://www.spur.org/publications/spur-report/2012-02-01/safe-enough-stay > (Sept. 1, 2014).

UBC (1973). "Uniform building code 1973 edition." UBC 73, International Conference of Building Officials, Whittier, CA.

Wang, C. and Blackmore, J. (2009). "Resilience Concepts for Water Resource Systems." *ASCE Journal of Water Resources Planning and Management*, 116(8).

Figure 01
Click here to download Figure: Figure_01.pdf

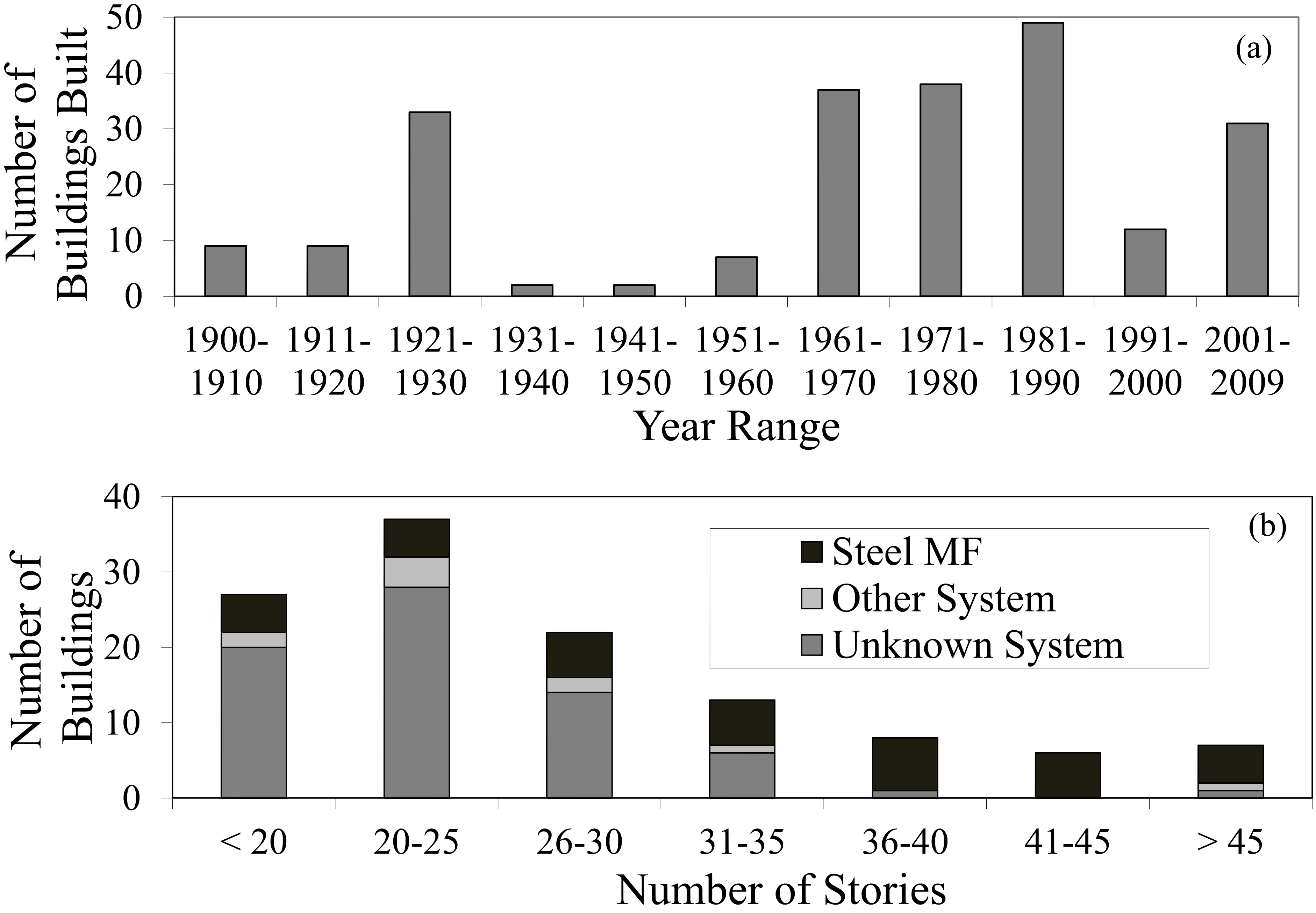

Figure 02
Click here to download Figure: Figure_02.pdf

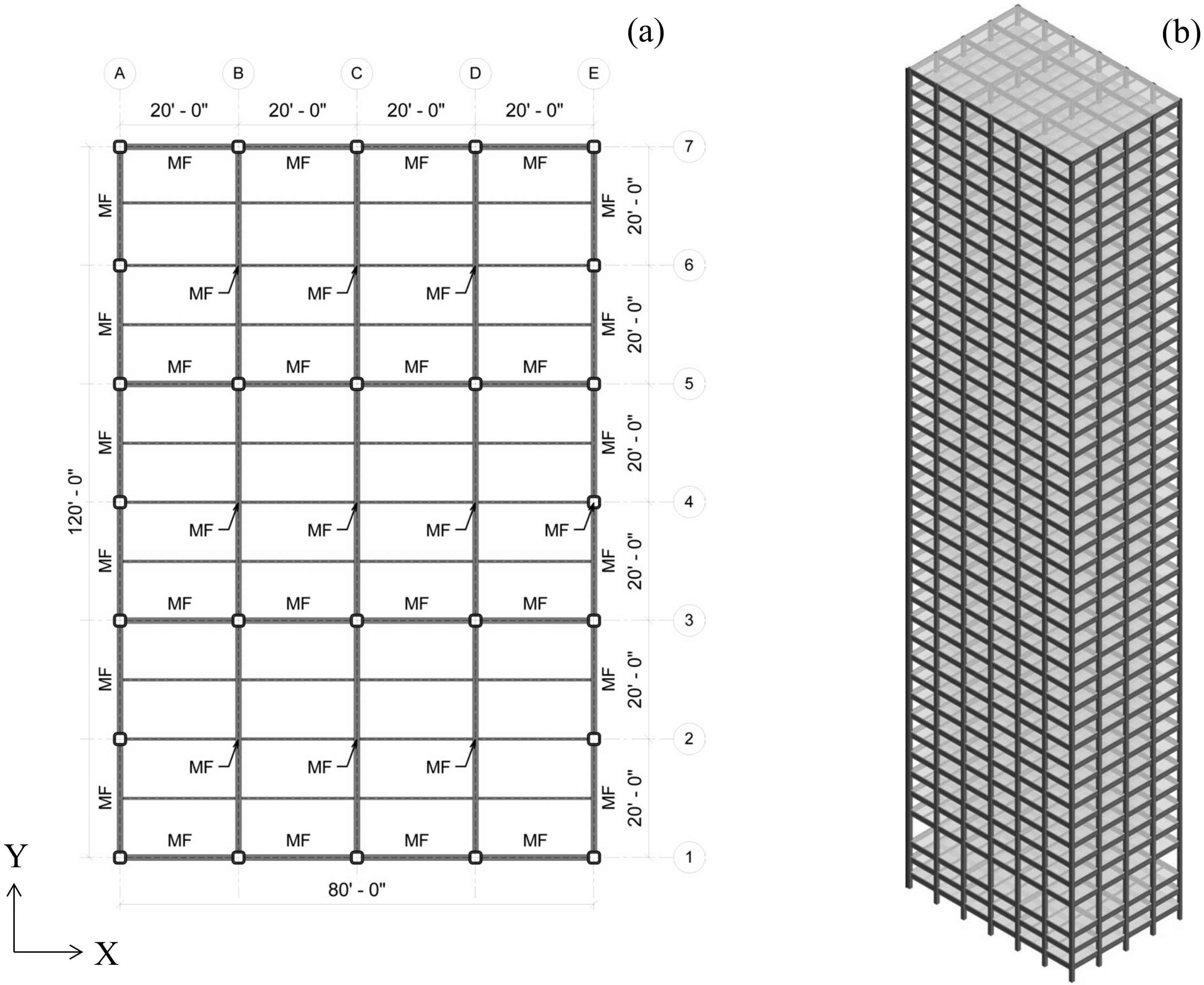

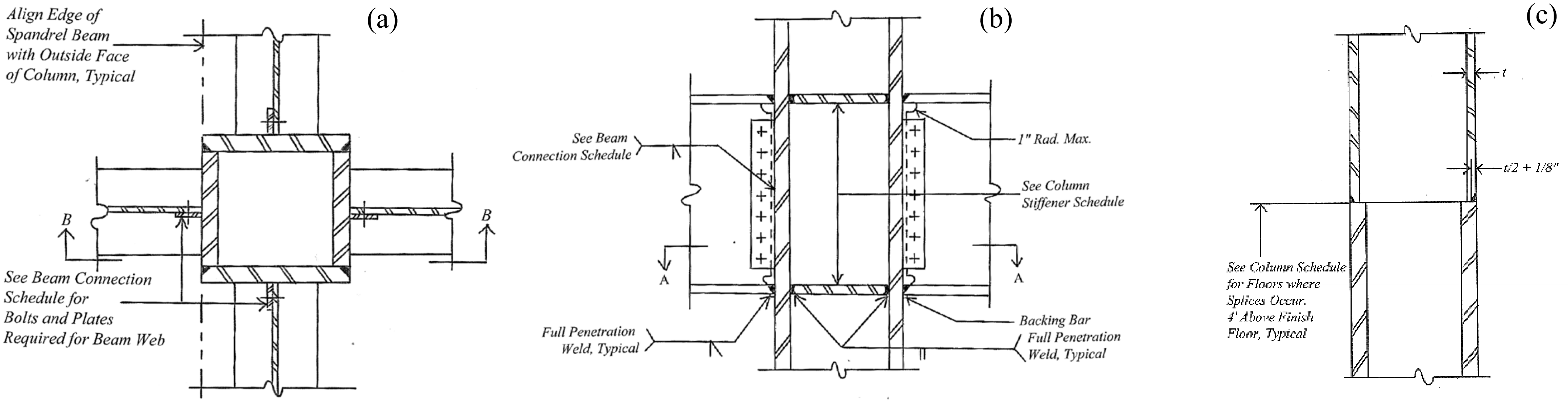

(a)
Align Edge of Spandrel Beam with Outside Face of Column, Typical
B
B
See Beam Connection Schedule for Bolts and Plates Required for Beam Web
(b)
See Beam Connection Schedule
1" Rad. Max.
See Column Stiffener Schedule
A
A
Backing Bar
Full Penetration Weld, Typical
Full Penetration Weld, Typical
(c)
t
t/2 + 1/8"
See Column Schedule for Floors where Splices Occur. 4' Above Finish Floor, Typical

Figure 04
Click here to download Figure: Figure_04.pdf

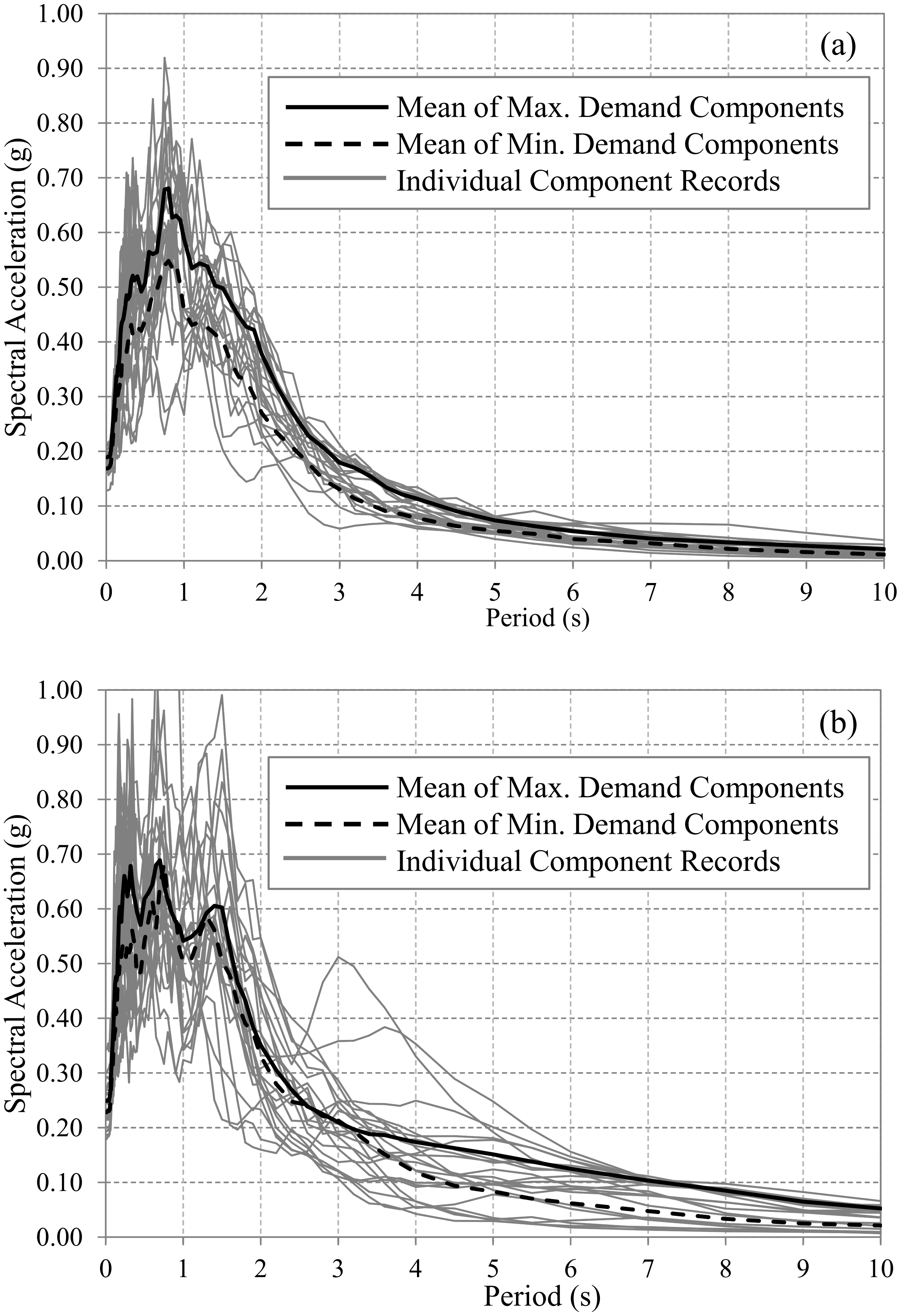

Figure 05
Click here to download Figure: Figure_05.pdf

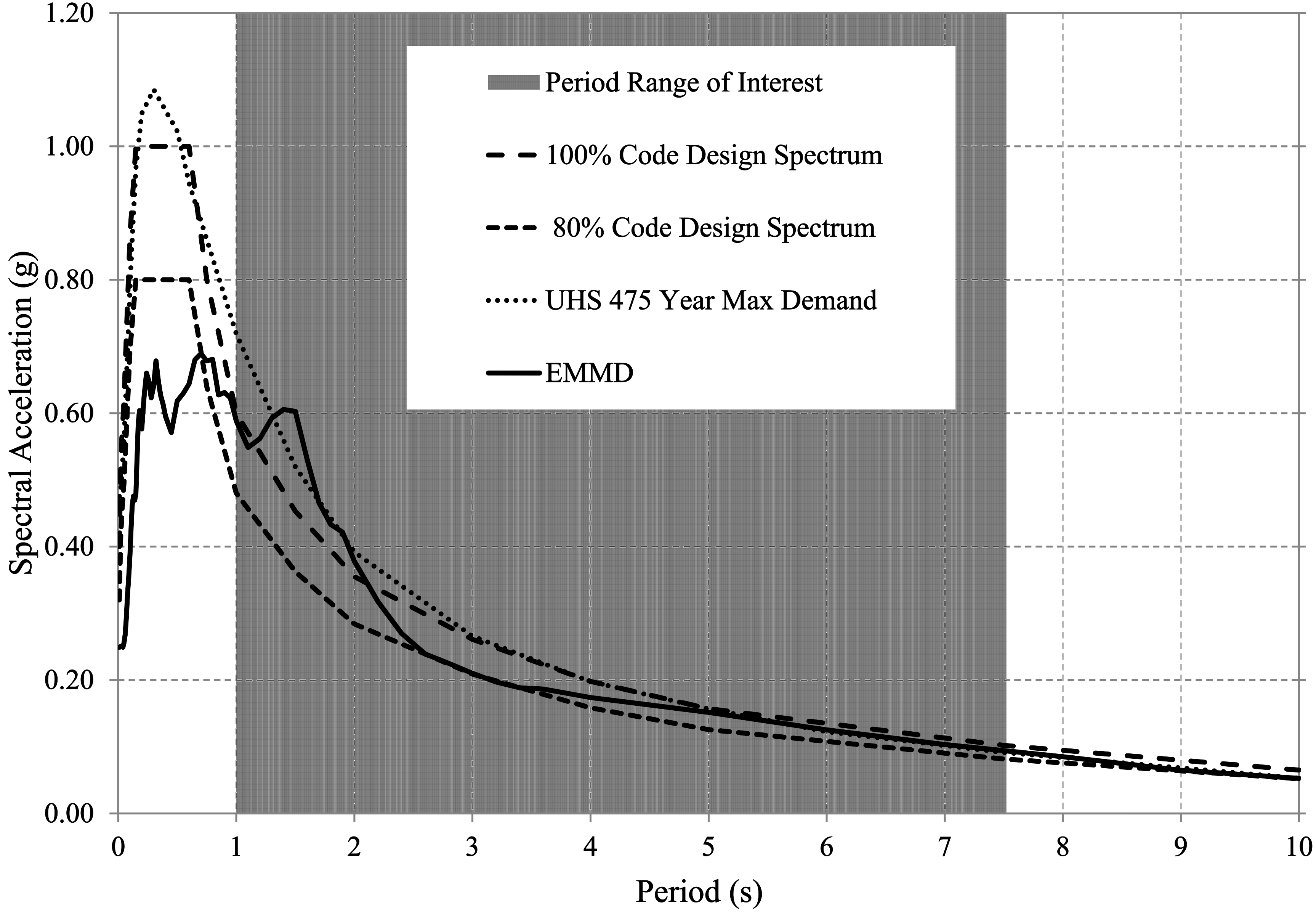

Figure 06

Click here to download Figure: Figure_06.pdf

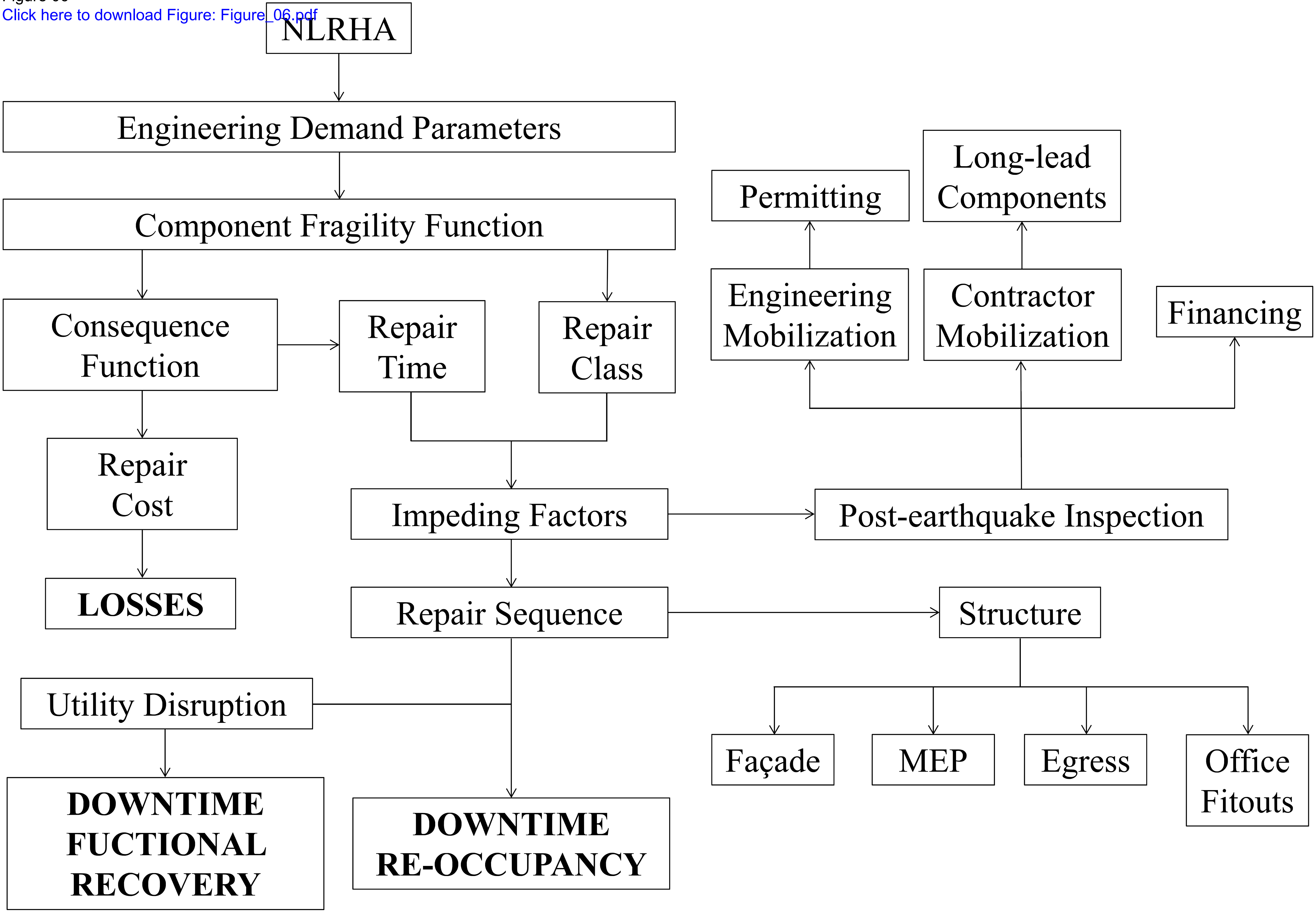

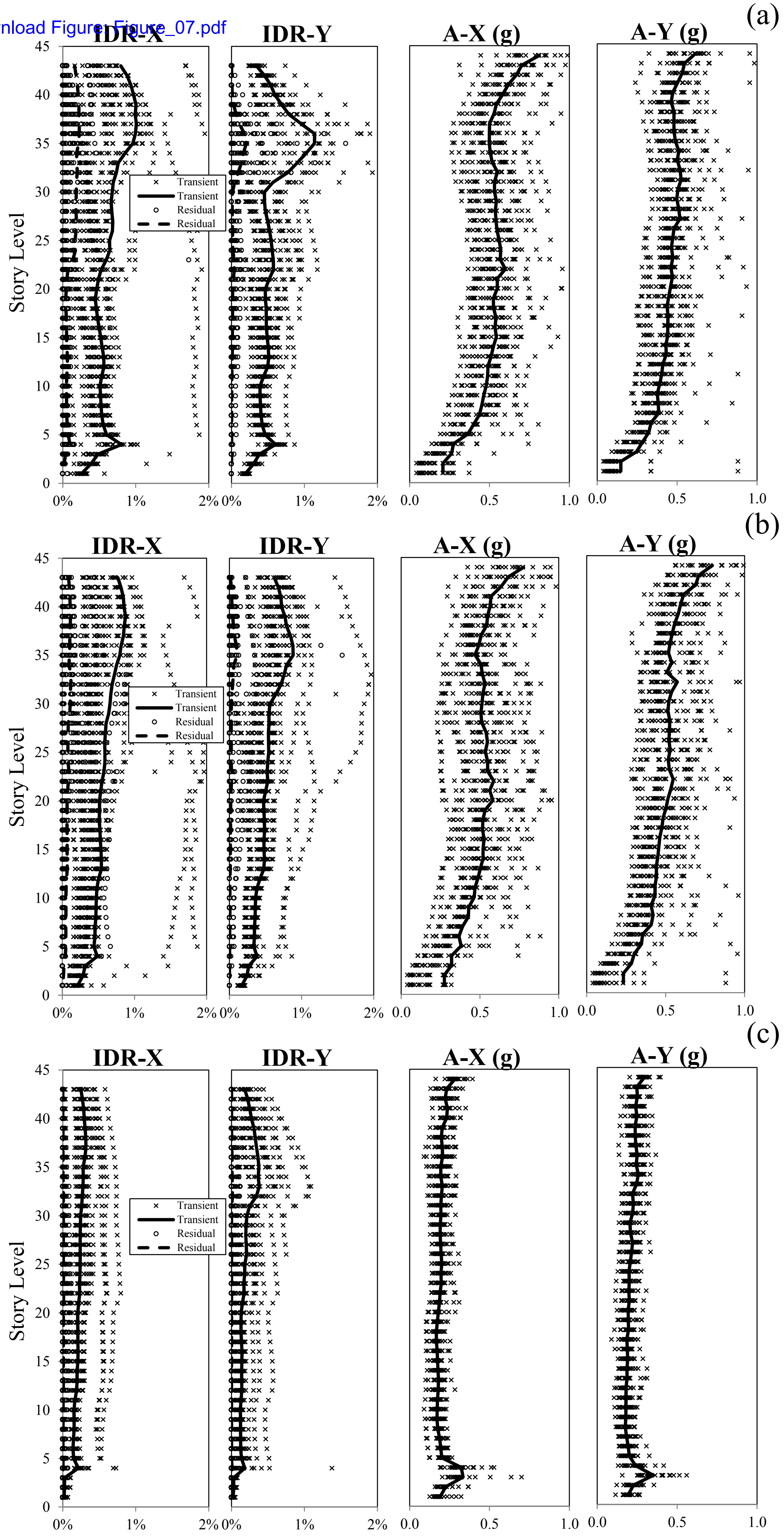
(a)
(b)
(c)
IDR-X
IDR-Y
A-X (g)
A-Y (g)
Story Level
Transient
Transient
Residual
Residual
0%
1%
2%
0.0
0.5
1.0
0
5
10
15
20
25
30
35
40
45

Figure 08

Click here to download Figure: Figure_08.pdf

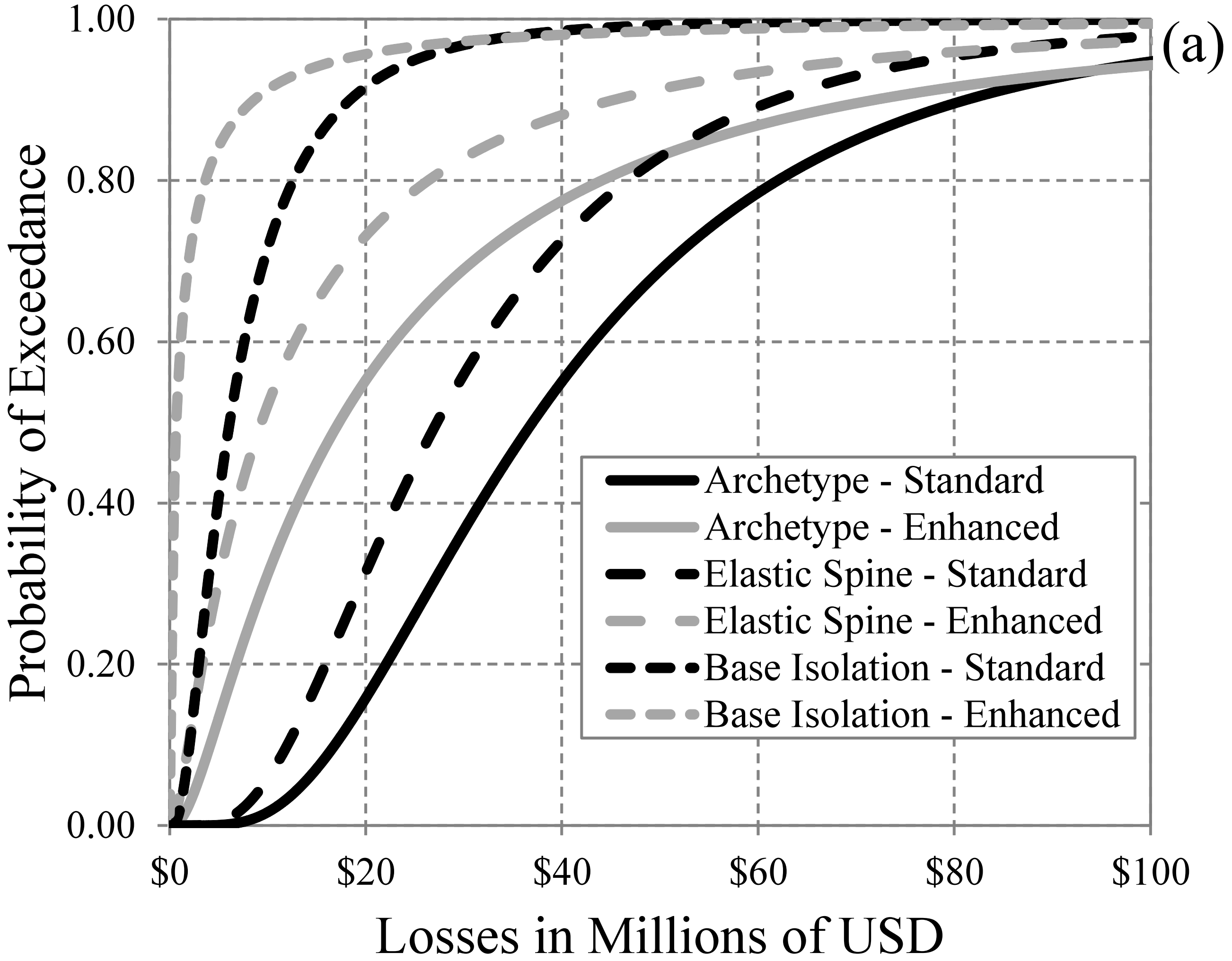

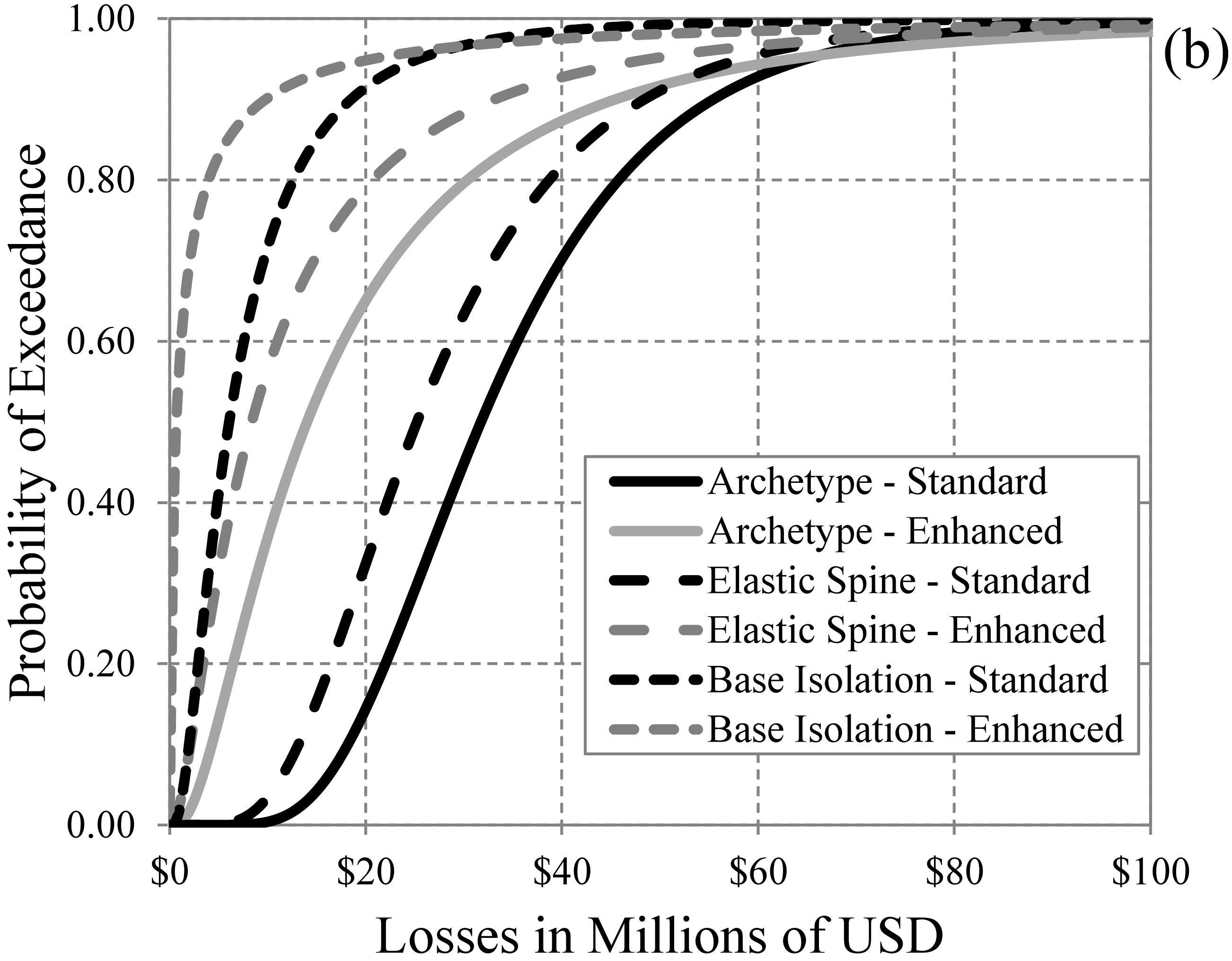

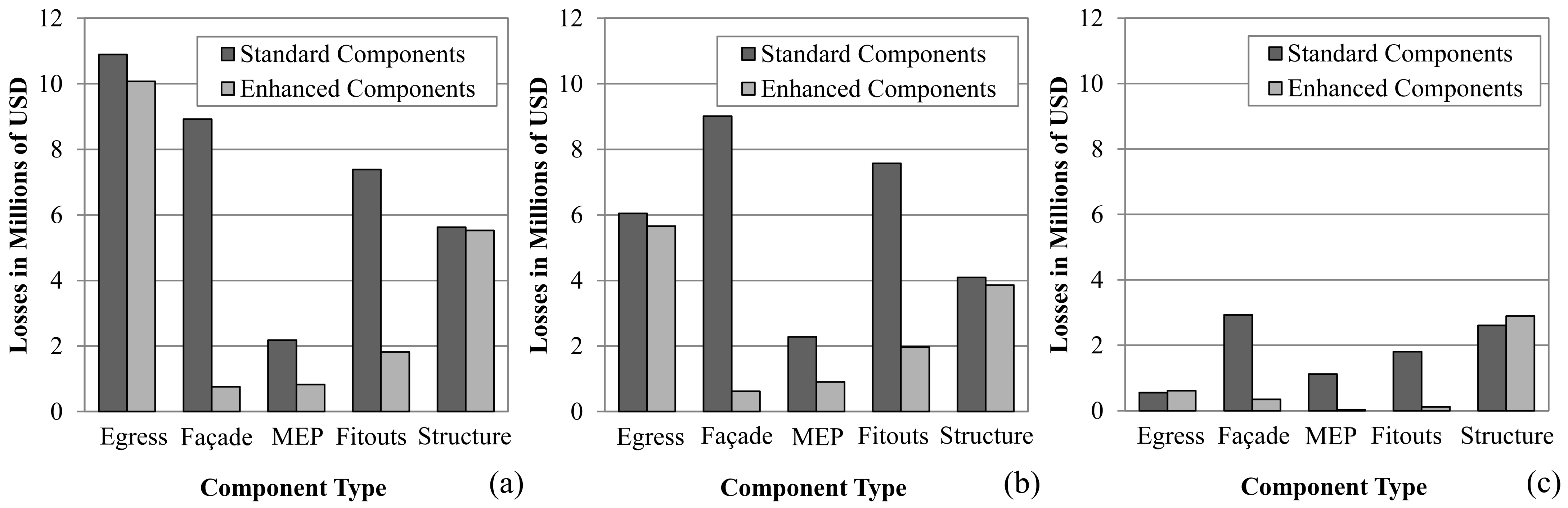
Standard Components
Enhanced Components
Losses in Millions of USD
0
2
4
6
8
10
12
Egress
Façade
MEP
Fitouts
Structure
Component Type
(a)
(b)
(c)

Figure 10
Click here to download Figure: Figure_10.pdf

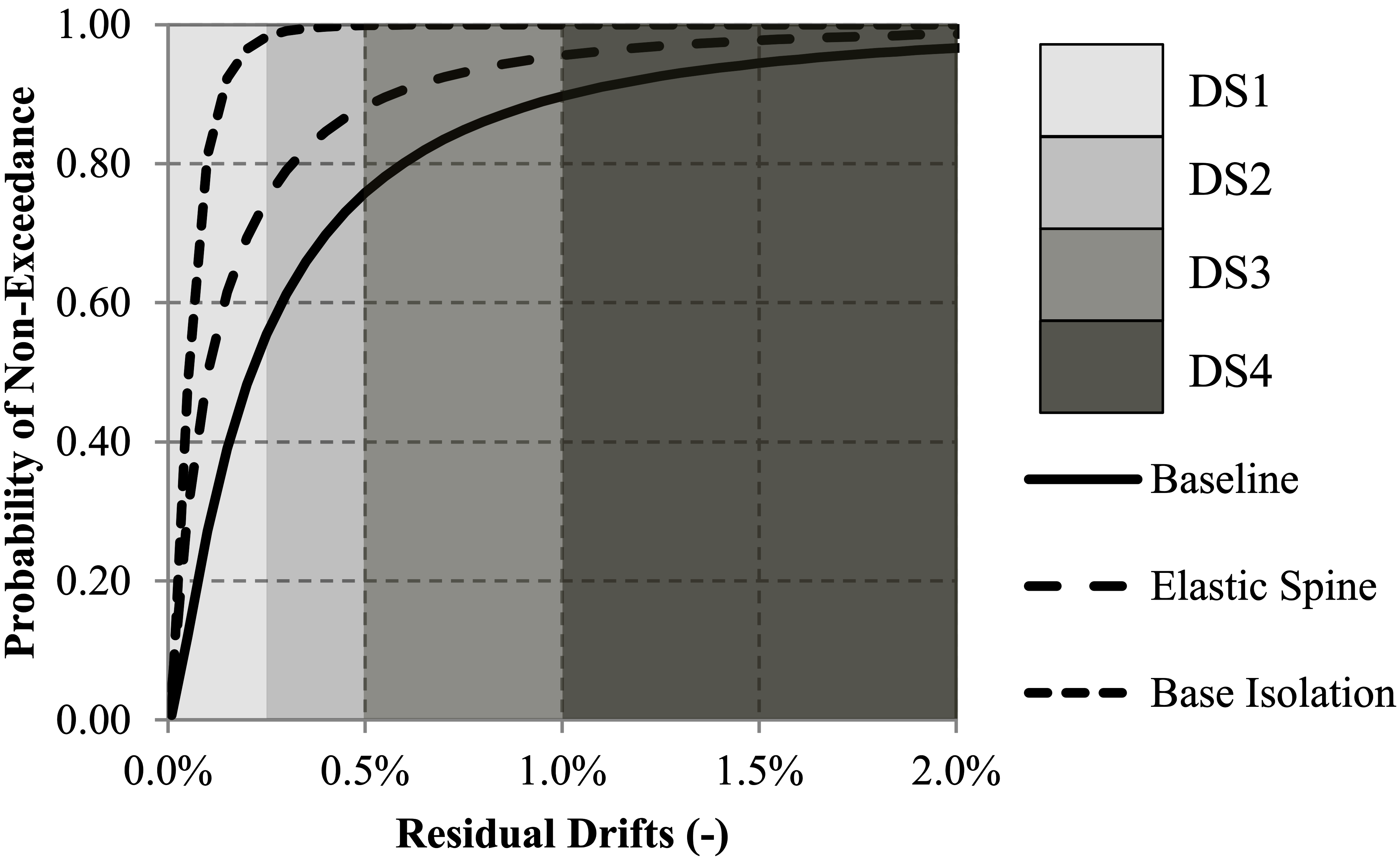

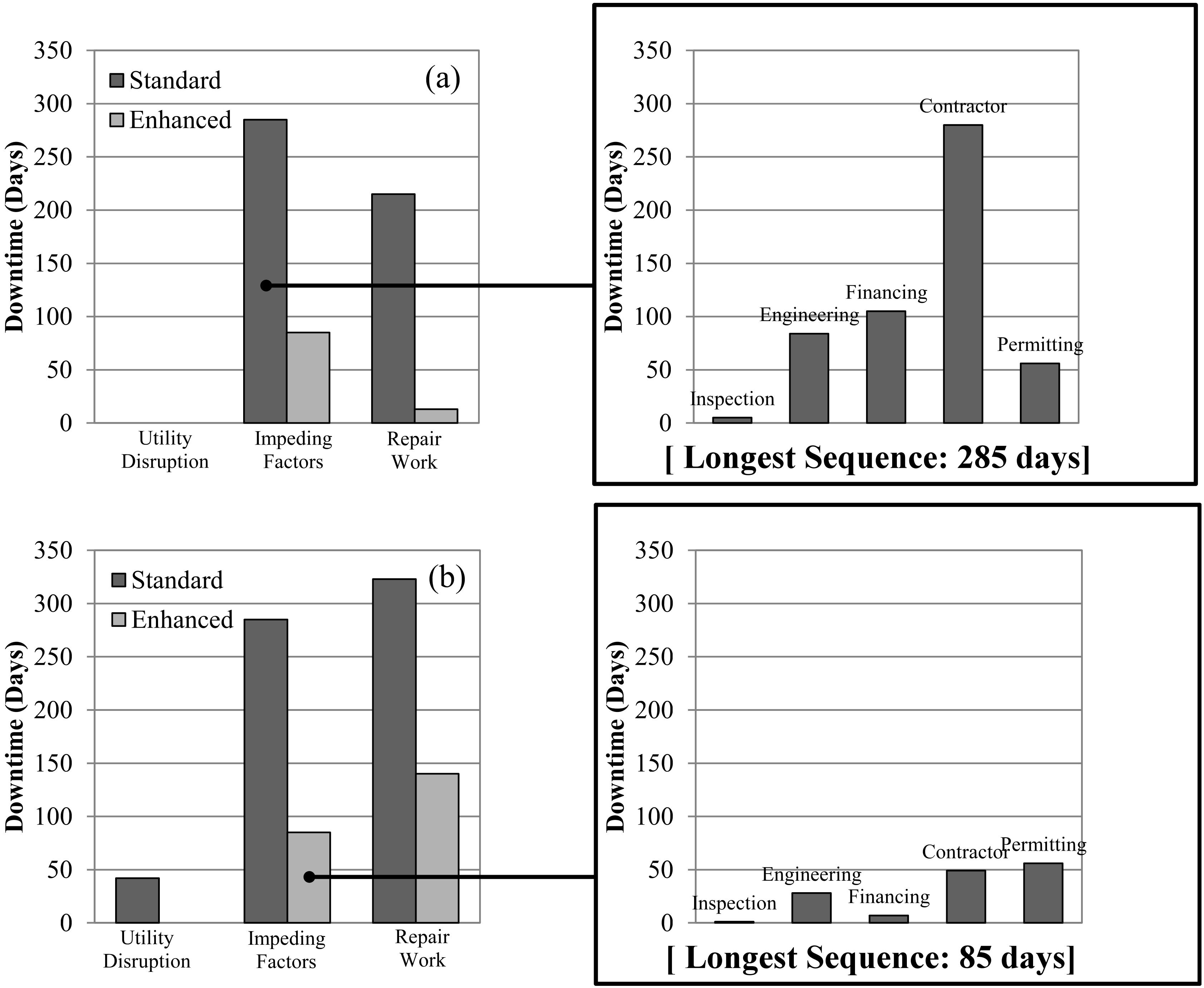
350
300
250
200
150
100
50
0
Downtime (Days)
Standard
Enhanced
(a)
Utility Disruption
Impeding Factors
Repair Work
Contractor
Financing
Engineering
Permitting
Inspection
[Longest Sequence: 285 days]
(b)
[Longest Sequence: 85 days]

Fig 1. Number of tall buildings built in San Francisco per decade between 1900 and 2010 (a) and lateral system types for tall buildings built between 1960 and 1990 (b).

Fig 2. Prototype 40-story office building plan (a) and isometric (b).

Fig 3. Typical details observed in existing building drawings: plan section of typical moment connection (a), elevation of typical moment connection (b) and typical splice (c).

Fig 4. Mean of maximum and minimum demand response spectra and individual components for short (a) and long (b) period suites of ground motions.

Fig 5. Compliance with ASCE 7-10 for site specific ground motions.

Fig 6. Loss and downtime assessment methodology. Adapted from REDi.

Fig 7. Demand parameters for the archetype building (a), elastic spine retrofit scheme (b) and base isolated retrofit scheme (c): transient and residual drifts (IDR) and accelerations (A) at each story in each building direction.

Fig 8. Loss estimates for archetype building (baseline), elastic spine and base isolation schemes with standard and enhanced non-structural components with (a) and without (b) consideration of residual drifts.

Fig 9. Contribution to losses of building components for archetype building (a), elastic spine retrofit (b) and base isolated retrofit (c) with standard and enhanced non-structural components.

Fig 10. Probability distribution of residual drifts for archetype building (baseline), elastic spine and base isolation retrofit schemes and associated damage states per FEMA P-58 (2012).

Fig 11. Downtime contributors for re-occupancy (a) and functional recovery (b) and sample disaggregation of impeding factors for the archetype building using standard non-structural components and no mitigation measures to minimize impeding factors versus enhanced non-structural components and mitigation measures to minimize impeding factors.